sustainability

MDPI

Article

Optimized Power Management Approach for Photovoltaic Systems with Hybrid Battery-Supercapacitor Storage

Djamila Rekioua [1], Khoudir Kakouche [1], Abdulrahman Babqi [2], Zahra Mokrani [1], Adel Oubelaid [1], Toufik Rekioua [1], Abdelghani Azil [1], Enas Ali [3], Ali H. Kasem Alaboudy [4] and Saad A. Mohamed Abdelwahab [4,*]

[1] Laboratoire LTII, Université de Bejaia, Bejaia 06000, Algeria; djamila.ziani@univ-bejaia.dz (D.R.); khoudir.kakouche@univ-bejaia.dz (K.K.); mokrani-zahra@hotmail.fr (Z.M.); adel.oubelaid@univ-bejaia.dz (A.O.); toufik.rekioua@univ-bejaia.dz (T.R.); azil.ghani@gmail.com (A.A.)
[2] Department of Electrical Engineering, College of Engineering, Taif University, Taif 21944, Saudi Arabia; ajbabqi@tu.edu.sa
[3] Faculty of Engineering and Technology, Future University in Egypt, New Cairo 11835, Egypt; enas.ali@fue.edu.eg
[4] Electrical Department, Faculty of Technology and Education, Suez University, Suez 43533, Egypt; ali.alaboudy@ieee.org
* Correspondence: saad.abdelwahab@suezuniv.edu.eg

Abstract: The paper addresses the ongoing and continuous interest in photovoltaic energy systems (PESs). In this context, the study focuses on an isolated photovoltaic system with hybrid battery-supercapacitor storage (HBSS). The integration of supercapacitors (SCs) in this system is particularly important because of their high specific power density. In photovoltaic (PV) systems, multi-storage systems use two or more energy storage technologies to enhance system performance and flexibility. When batteries and supercapacitors are combined in a PV system, their benefits are maximized and offer a more reliable, efficient, cost-effective energy storage option. In addition, effective multi-storage power management in a PV system needs a solid grasp of the energy storage technologies, load power demand profiles, and the whole system architecture. This work establishes a battery-supercapacitor storage system (HBSS) by combining batteries and supercapacitors. The primary objective is to devise a novel management algorithm that effectively controls the different power sources. The algorithm is designed to manage the charge and discharge cycles of the hybrid battery-supercapacitor energy storage system (HBSS), thereby guaranteeing that the state of charge (SOC) for both batteries and supercapacitors is maintained within the specified range. The proposed management algorithm is designed to be simple, efficient, and light on computational resources. It efficiently handles the energy flow within the HBSS, optimizing the usage of both batteries and supercapacitors based on real-time conditions and energy demands. The proposed method ensures their longevity and maximizes their performance by maintaining the SOC of these energy storage components within the specified limits. Simulation results obtained from applying the management strategy are found to be satisfactory. These results show that the proposed algorithm maintains the SOC of batteries and supercapacitors within the desired range, leading to improved energy management and enhanced system efficiency.

Keywords: batteries; hybrid energy storage; photovoltaic; power management control; supercapacitor

check for updates

Citation: Rekioua, D.; Kakouche, K.; Babqi, A.; Mokrani, Z.; Oubelaid, A.; Rekioua, T.; Azil, A.; Ali, E.; Alaboudy, A.H.K.; Abdelwahab, S.A.M. Optimized Power Management Approach for Photovoltaic Systems with Hybrid Battery-Supercapacitor Storage. *Sustainability* **2023**, *15*, 14066. https://doi.org/10.3390/su151914066

Academic Editor: Francesco Riganti Fulginei

Received: 5 August 2023
Revised: 9 September 2023
Accepted: 18 September 2023
Published: 22 September 2023

Copyright: © 2023 by the authors. Licensee MDPI, Basel, Switzerland. This article is an open access article distributed under the terms and conditions of the Creative Commons Attribution (CC BY) license (https://creativecommons.org/licenses/by/4.0/).

1. Introduction

In remote areas, the adoption of renewable energy systems is rising [1,2]. In order to keep the source energy and the charge demand in an optimal power balance, the energy storage system is essential [3,4]. In photovoltaic (PV) systems, energy storage is used to store excess solar energy produced during the day so that it can be used at a later time when the sun is not shining or when electricity demand is high. Several types of storage technologies are used in photovoltaic (PV) systems, including batteries, supercapacitors, Flywheels, pumped hydroelectric storage, thermal energy storage and fuel cells. Batteries

are the most used storage for PV systems, as they are relatively inexpensive and can be easily installed in residential and commercial settings [5,6]. Supercapacitors, or ultracapacitors, store electrical energy as an electrostatic charge. They have a high-power density, meaning they can charge and discharge quickly, making them well-suited for applications that require high power output. While supercapacitors have some advantages over batteries, such as faster charging times and longer lifetimes under certain conditions; they also have some limitations that may make them less practical for some PV system applications [7]. The drawbacks are low energy density, high cost, limited lifespan, voltage limitations, and leakage current [8,9].

The system requirements and the resources at hand will determine the best combination. It will be determined by various criteria, including the system's precise requirements, the available budget, and the tradeoffs between the advantages and downsides of each technology. The combination of batteries and supercapacitors has various advantages. Batteries can store significant quantities of energy for extended periods, but supercapacitors may discharge fast and give high-power bursts for brief periods. This combination has the potential to assist with balancing the load on the PV system, particularly during high-energy-demand periods. When a PV system produces extra energy, the batteries may be charged, and when power demand is high, the stored energy in the batteries can be released. However, batteries have a limited discharge rate and are susceptible to voltage loss during high-power demands. Supercapacitors, however, discharge fast, giving extra power to meet high power demands, and they can also maintain a constant voltage output during periods of high-power demand. Combining batteries and supercapacitors has the added benefit of extending the life span of both power sources. Supercapacitors can absorb high power bursts, lowering battery burden and reducing battery cycling. It prevents battery damage, increasing their life span. Supercapacitors are more costly than batteries, but they can reduce the capacity required for the battery system. However, there are some potential disadvantages, such as higher costs, complex control systems, maintenance issues, safety concerns, and limited scalability.

Power management of multi-storage in a PV system is critical to ensuring that the various energy storage technologies perform successfully and efficiently together. Additionally, continuous monitoring of the SOC ensures that the storage systems operate within their optimal range, by ensuring optimized utilization and maximum system efficiency [10–12]. Power management of photovoltaic (PV) systems with multi-storage technologies has been the subject of several research papers [13–15]. The power management of PV systems with multi-storage technologies involves controlling the power flow between different storages while ensuring that the load is supplied [16–19]. The goal is to optimize the use of each storage technology and maximize the overall system efficiency.

SCs are compared to other storage devices [20–22], and the advantages of hybrid PV-battery SCs systems are researched [23,24]. Furthermore, some studies [25–27] propose hybrid energy storage systems (HESS) as a feasible approach, as photovoltaic-battery supercapacitors or fuel cells. Most research with these hybrid systems focuses on load control and demand sharing. Ref. [28] combines batteries and supercapacitors to optimize electric vehicle operation across a wide range of ambient temperatures. This hybrid system likely utilizes the inherent strengths of both technologies—batteries for higher energy storage capacity and supercapacitors for quick energy delivery and management of power spikes. To optimize the performance of these hybrid systems, advanced control strategies like model predictive control are employed [29].

Electric vehicles' energy management systems are critical components, as they determine how energy is sourced, stored, and utilized to optimize efficiency and performance. Battery/supercapacitor systems combine the high energy density of batteries with the fast charging and discharging capabilities of supercapacitors, making them suitable for addressing the varying power demands of electric vehicles [30]. In [31], the authors present an economic strategy for grid-connected wind power systems using a battery–supercapacitor system. It provides insights into the technical aspects of the economic dispatch approach

and may present simulation or experimental results to showcase the effectiveness of their strategy in achieving economic efficiency and grid stability. In [32], the authors explore the performance and analysis of photovoltaic (PV) systems when integrated with energy storage systems. Storage systems play a vital role in enhancing the effectiveness and reliability of PV systems by addressing the intermittency of solar energy generation and varying energy demands.

By increasing the effectiveness and viability of photovoltaic energy systems, reducing dependency on non-renewable energy sources, and promoting technological improvements in energy storage and management, this study contributes to sustainability. It presents an innovative power management technique that combines battery and supercapacitor storage technologies to increase the effectiveness and sustainability of photovoltaic (PV) systems. First, by improving the power management strategy for these systems, the research may help to improve the overall effectiveness of converting solar energy into usable electricity. A stable and reliable energy supply also depends on effectively controlling the energy storage and discharge cycles. An optimal strategy can minimize waste and associated environmental impacts by maximizing the useful life of the storage components and limiting the need for frequent replacements. Peak demand shifting is a crucial power management component in PV energy systems.

Also, employing effective power management techniques enables PV systems to run independently or with little dependence on the grid. It can improve access to electricity and reduce the environmental effects of grid development. It can be especially helpful in isolated or off-grid areas. Finally, a storage device using a mix of batteries and supercapacitors suggests technological advancement. The creation and improvement of such systems may result in improvements to energy storage that are more effective, durable, and environmentally friendly. Publication of research papers like this one allows researchers and practitioners to access valuable knowledge on sustainable energy solutions.

We introduce in this study a PMC that permits the control of the charge and discharge process of storage. The application is demonstrated in Bejaia, an area with a significant potential for solar irradiation, using four different day patterns. The validity and usefulness of the suggested power management approach are shown in this study through simulation results. Several experimental tests were carried out on a real-time simulator (RT-LAB) to assess the suggested control algorithms.

2. Brief State of Art

To address solar energy limits, particularly in remote areas, hybrid systems with different storage sources or multi-storage might be used [33], but power management controls (PMC) are necessary to control the various powers. The strategies vary according to the type of energy system. Furthermore, it works to coordinate the numerous sources, allowing the power or energy created to be controlled. Many articles have looked into these control strategies. Despite the fact that the technologies used in each vary, the majority of applications focus on isolated systems for electrification [34,35], microgrids [36,37], and multi-storage in traction and electric cars [38,39]. Various algorithms in the literature can address this problem [38–55]. Some EMs approaches make use of analogical statements in decision algorithms [40] or linear controllers such as in [39]. Others use smarter [41] and more predictive techniques [36,37,42,43]. Olatomiwa, L. et al. [44] comprehensively analyzed energy management strategies based on fuzzy logic systems. The authors of paper [45] reviewed many techniques for using extra energy in renewable systems, which are generally unused. They provide many strategies for improving functioning without incurring additional costs. In another study [46], the EMS is used to derive the optimal control signals. The application was created for stand-alone DC microgrids. This strategy provides for ideal values, a realistic simulation duration, and increased battery life, while lowering overall installation costs by removing dump loads. Meng et al. [47] summarize the many approaches utilized for microgrids (MG) and conclude that these controls are a multi-objective topic that deals not only with electrical issues but also with economic and

environmental factors. Another study [48] reveals that energy management optimization is used with sizing algorithms to reduce system costs. In [49], the authors propose a hybrid renewable energy system based on grid-integrated storage technology. Fuzzy controllers (FLC) were used in the optimization and design technique. The FLC was also utilized in [50] to control the total power supply of the flow system while keeping the charging battery in an operable state. In [51–53], it presented a PMC for electric vehicles (EV) that does not employ power optimization but accounts for and manages extra power using a multi-objective approach. The approach was then extended to a pumping system with many sources [54].

In this regard, this research aims to increase the performance of a standalone photovoltaic system with multi-storage (batteries/supercapacitors). The strategy considers the SOC and charging/discharging current of the batteries and SCs for SOC balancing-based power sharing through power converters. The batteries and SCs and photovoltaic systems are linked to DC bus via DC-DC converters, which enable improving the dynamic efficiencies of the system through the regulation of batteries and SCs charging/discharging as a function of the EMS provided when the system is exposed to variable perturbations. The contribution of this paper consists of providing simple implementations of power flow management regarding optimal energy flow between PV system, batteries and SCs system, and load. Balancing between minimal energy flows through the connecting line with minimal requirements of batteries and SCs capacity is kept. The real-time simulation/experimentation that uses MATLAB/Simulink and RT-LAB is realized to confirm the effectiveness of the designed EMS and control strategy by comparing the findings with those of other authors. The rest of this article is organized as follows: The proposed PV hybrid storage systems are defined in Section 3. Section 4 presents parameters identification and modelling of the different subcomponents. Section 5 is devoted to the proposed power management control. The studied system is simulated under MATLAB/Simulink to verify the suggested control and energy management technique. The findings are presented in Section 6. On a real-time simulator (RT-LAB), a number of experimental tests were carried out to assess the suggested control algorithms. Section 7 describes the step description, and the results are compared to the simulation results to demonstrate the usefulness of the proposed system. Finally, Section 8 provides the conclusion summarizing this article's contributions.

3. Proposed PV Hybrid Storage System

PV panels, a DC/DC converter, and a (battery/supercapacitor) storage system are all components of the system under study (Figure 1). Long-term energy storage is possible with battery technology. Supercapacitors can quickly absorb current variation, lowering the risk to the batteries. The voltage of the solar panels can be raised by connecting a boost converter to them. Due to the connection of supercapacitors and batteries to the DC bus, all powers can supply the load simultaneously.

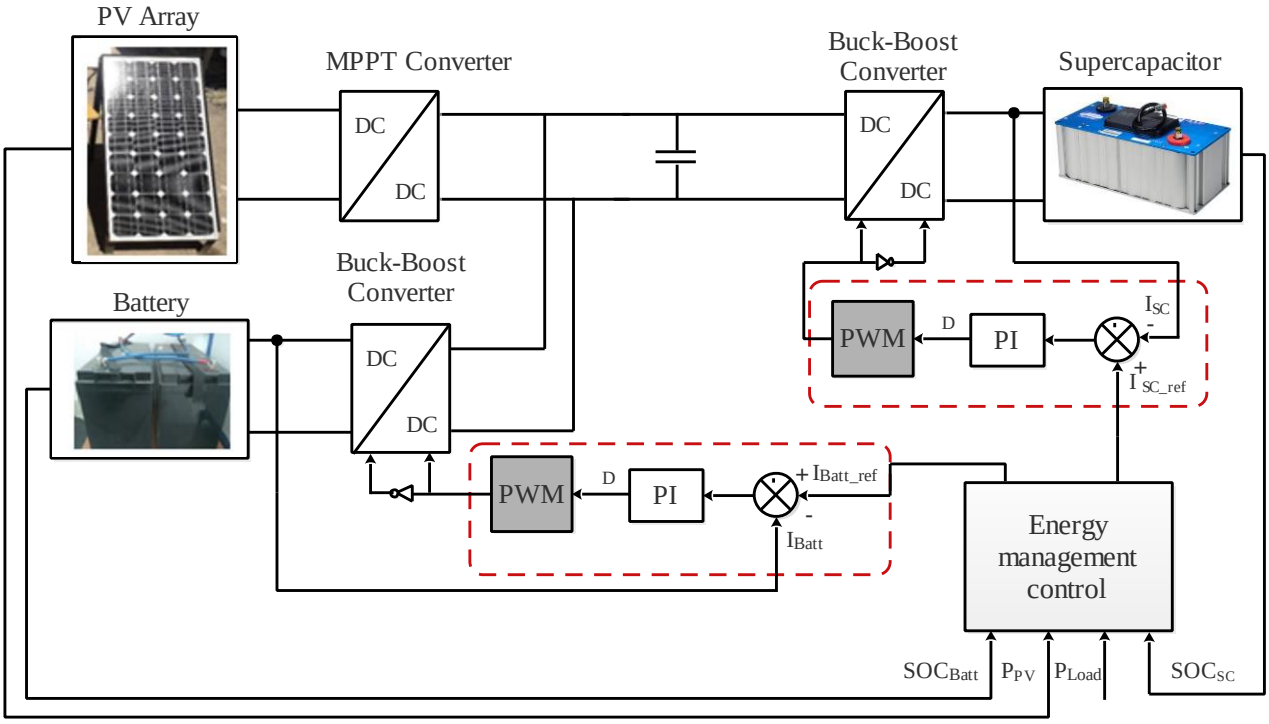


Figure 1. Proposed PV based hybrid storage scheme.

4. Parameters Identification and Modelling

4.1. Photovoltaic Pannel Modeling

A multitude of models are used to compute PV panel electrical curves. Their level of accuracy and complexity varies. We applied the one-diode model in our research [40,54]. Although simple, it is useful for characterizing the electrical properties of a solar generator (Figure 2).

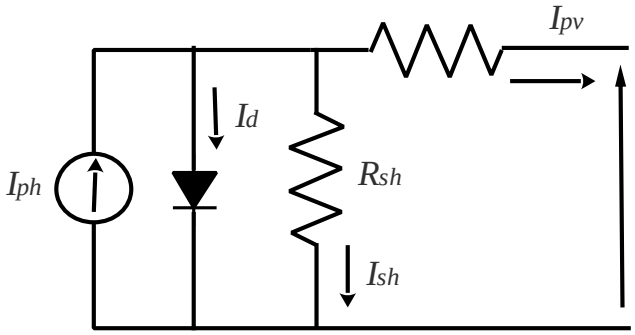


Figure 2. One-diode model.

The electrical current can be written as [40,54]:

$$I_{pv} = I_{ph} - I_d - I_{sh} \quad (1)$$

$$I_{pv} = I_{ph} - I_0\left[\exp\left(\frac{V_{pv} + R_s \cdot I_{pv}}{A \cdot V_{th}}\right) - 1\right] - \frac{V_{pv} + R_s \cdot I_{pv}}{R_{sh}} \quad (2)$$

I_{ph}, I_d, I_{sh} are, respectively, the photocurrent, diode current, and shunt current, R_{sh} is the shunt resistance, and R_s is the serial resistance.

Various tests are performed to identify the different PV panel characteristics (Figure 3) under three distinct solar irradiation and ambient temperature levels: low, medium, and high as pointed out in Table 1.

Table 1. PV identification tests.

Tests	Es (W/m^2)	Ta (°C)
Test 1	750.00	28.00
Test2	410.00	27.50
Test 3	158.00	21.00



Figure 3. Experimental test bench.

The established experimental bench is highlighted in Figure 4. It is composed by an 80 Wp panel (Table 2), a voltmeter, and an amperemeter with a variable load. The ambient temperature and solar irradiance are measured by using measurement devices.

Table 2. Parameters of the photovoltaic panel 80 Wp.

Parameters	Values
photovoltaic power P_{pv}	80 W_p
maximum current at PPM I_{mpp}	4.65 A
maximum voltage at PPM V_{mpp}	17.5 V
short circuit current I_{sc}	4.95 A
open circuit voltage V_{oc}	21.9 V
temperature coefficient of short-current α_{sc}	3 mA/°C
voltage temperature coefficient of short-current β_{oc}	−150 mV/°C

In the lab, sun radiation and temperature were measured using measurement acquisition equipment (Figure 5). To test the effectiveness of the proposed energy management strategy, extensive numerical simulations were made under Matlab/Simulink environment. Runge–Kutta of fourth order is used as a solver with a step of 1×10^{-5}. Table 3 below summarizes the used simulation details.

Table 3. Parameters simulation details.

Parameters	Value
D	96 days
T_s	1×10^{-4}
Solver	RK-ode4
Solver type	Fixed

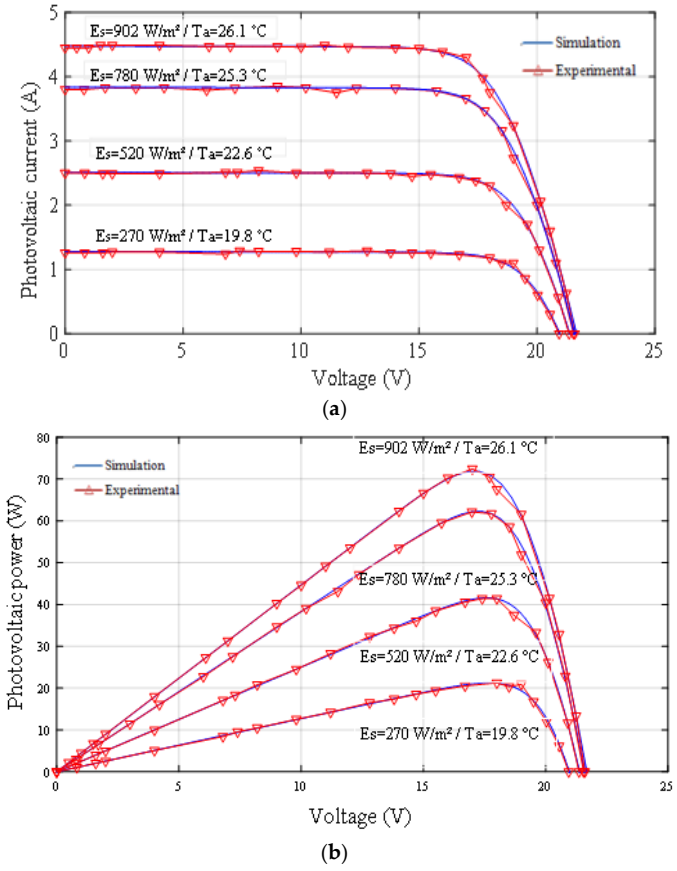


Figure 4. Electrical characteristics. (**a**) $I_{pv} = f(V_{pv})$; (**b**) $P_{pv} = f(V_{pv})$.



Figure 5. Measurement acquisition device at the laboratory.

4.2. Battery Modeling

The following model (Figure 6) has been employed in our work using various voltage and charge state equations [51–53].

$$\begin{cases} V_{Batt} = E_0 - R_{Batt} \cdot I_{Batt} - k \cdot \int \left(\frac{I_{Batt}}{Q} \right) \cdot dt \\ SOC = 1 - \frac{I_{Batt} \cdot t}{C_{Batt}} \end{cases} \quad (3)$$

In this study, a 12 V–100 Ah battery is used as a storage device as shown in Figure 7a. Identification is performed to determine the battery impedance (Z_{Batt}). Figure 7b shows the different curves obtained while proceeding to identify the battery. It shows that there exists a phase shift of 3 degrees between voltage and current (voltage is lagging).

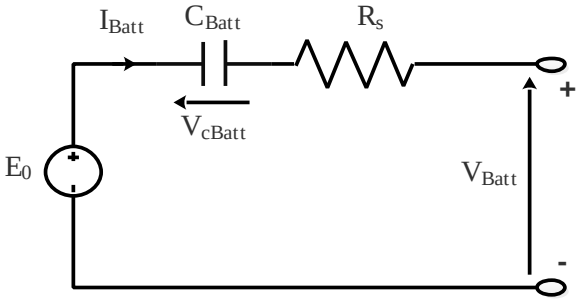
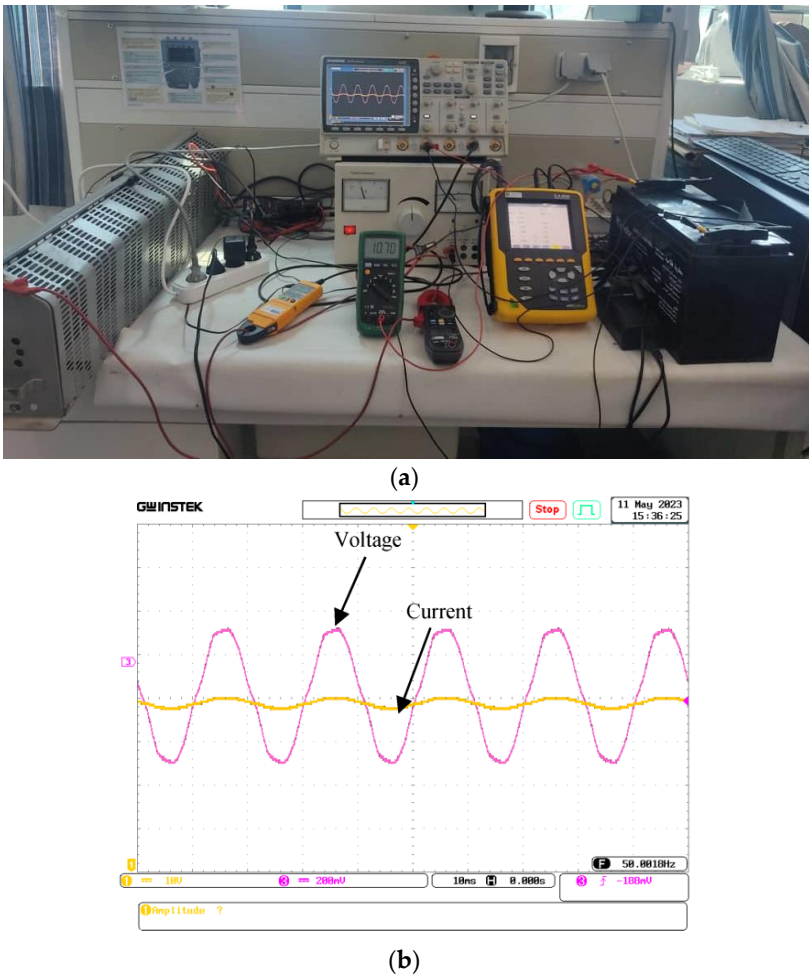


Figure 6. R-C model of the battery.



(**a**)

(**b**)

Figure 7. Battery identification. (**a**) Test bench; (**b**) battery voltage and current curves.

The phase shift of these two signals gives the impedance Z_{Batt}. And then internal resistance R_{Batt}, and the capacitive reactance X_{Batt}.

The absolute value of the battery's impedance is:

$$Z_{Batt} = R_{Batt} + jX_{batt} \tag{4}$$

$$\begin{cases} Z_{Batt} = \frac{U_{batt}}{I_{Batt}} \\ R_{Batt} = Z_{Batt} \cdot \cos\rho \\ X_{Batt} = Z_{Batt} \cdot \sin\rho \\ C_{Batt} = \frac{1}{(X_{Batt} \cdot 2 \cdot \pi \cdot f)} \end{cases} \tag{5}$$

with: f the frequency, (Hz).

The different calculated results are: R_{Batt} = 0.795 Ω, X_{Batt} = 0.07 Ω and C_{Batt} = 44.96 mF.

All of these identified variables were included in simulation models to establish realistic mathematical models that were as near to the experiment as possible.

4.3. Supercapacacitors Model

Different models for simulating a supercapacitor (SC) have been put forth in the literature [56,57]. The corresponding electric circuit with two RC branches (Figure 8) is the model utilized in our research.

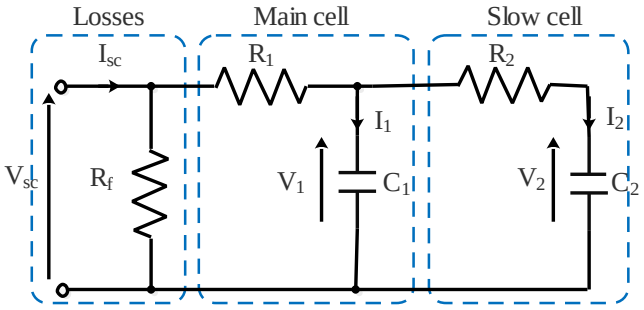


Figure 8. SC model.

There are two branches to it. The supercapacitor's immediate behavior during quick charge and discharge cycles within seconds is defined by the R_1C_1 branch. The sluggish branch is the second branch R_2C_2. The model is described by the equations below:

$$\begin{aligned} U_{sc} &= N_{sc-s} \cdot V_{sc} = N_{sc-s} \cdot (V_1 + R_1 \cdot I_{sc}) \\ &= N_{sc-s} \cdot \left(V_1 + R_1 \cdot \frac{i_{sc}}{N_{sc-p}} \right) \end{aligned} \tag{6}$$

The secondary capacity C_2's secondary voltage V_2 is determined by:

$$\begin{aligned} V_2 &= \frac{1}{C_2} \int i_2(t) \cdot dt \\ &= \frac{1}{C_2} \int \frac{1}{R_2} (v_1 - v_2) \cdot dt \end{aligned} \tag{7}$$

Q_2 is the instantaneous charge of C_2, we have:

$$Q_2 = \int i_2(t) \cdot dt \tag{8}$$

The current i_1 in the main capacitor C_1 is given as:

$$i_1 = i_{sc} - i_2 \tag{9}$$

There are three main techniques to characterize a supercapacitor as listed in Table 4 shown below:

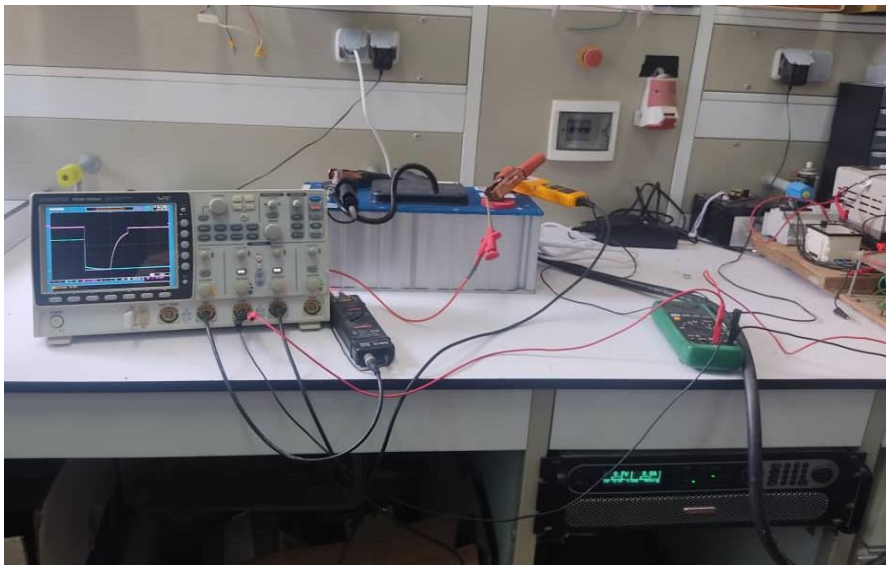
Table 4. Different supercapacitor identification techniques [58].

Technique	Description	Advantages	Drawbacks
Electrochemical impedance spectroscopy	Supercapacitor impedance is measured as a function of frequency	Identifies several supercapacitor electrical properties such as capacitance, resistance, and frequency-dependent behavior	Expensive equipment required.
Cyclic voltammetry	Various voltages are used to the supercapacitor and the current is measured.	Provides information about the supercapacitor's capacitance, charge/discharge behavior, and electrochemical stability.	High degree of interpretation and practical skills are required
Charge–Discharge Cycling	The capacitor is charged to a set voltage, then it is discharged through a load while measuring t voltage and current.	Fast and relatively easy way to determine the capacitance and resistance of supercapacitors	The accuracy of the results can be influenced by the quality of measurement equipments, the accuracy of the voltage and current measurements

These three methods are just a few of some others that can be used to describe supercapacitors. The exact properties of the supercapacitor being tested and the data needed for the application determine the technique to use. Charge–discharge cycling was employed in this study to evaluate the supercapacitor (Figure 9). During charge and for a current of 10 A, we obtain the following response (Figure 9a). The resistance R_1 is the cause of the drop in the load voltage at the initial moment. C_1 is determined directly from the constant current load characteristic of the cell (Figure 9b).

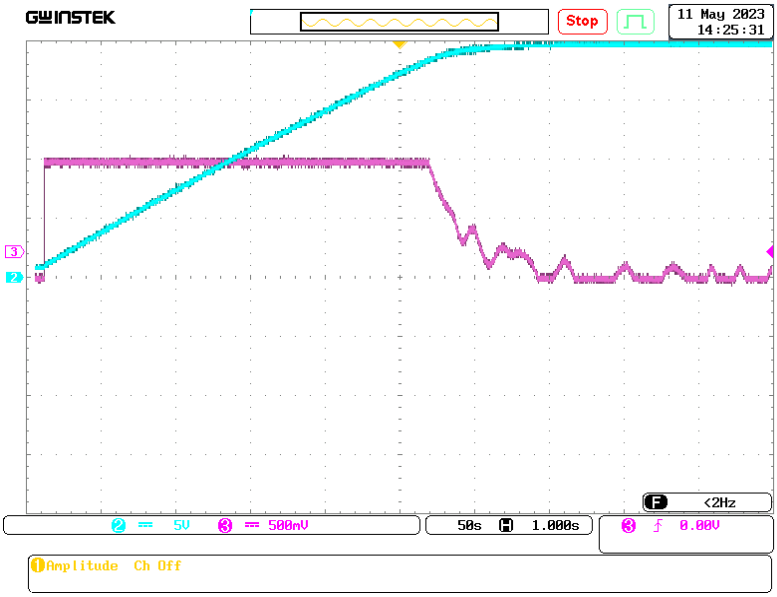
$$C_1 = \frac{I}{(\Delta V/\Delta t)} = \frac{10}{(20-2/300-10)} = 161F$$

Table 5 displays the various supercapacitors' researched parameters.



(**a**)

Figure 9. *Cont.*



(**b**)

Figure 9. Supercapacitor identification test bench. (**a**) Test bench;(**b**) tests under charge and discharge.

Table 5. Supercapacitor parameters.

Parameters	Values
Rated capacitance	165 F
Maximum ESR_{DC} initial	60 m Ω
Test current for capacitance and ESR_{DC}	100 A
Rated voltage	48 V
Stored energy	53 Wh
Absolute maximum voltage	51 V
Absolute maximum current	1900 A
Maximum series voltage	750 V
Capacitance of individual cells	3000 F
Storage energy, individual cell	3.0 Wh
Number of cells	18

The different identified parameters are shown in Table 6.

Table 6. Obtained identified parameters.

Parameters	Values
R_1	1.8 Ω
R_2	0.5 Ω
C_1	161 F
C_2	102 F

5. Proposed Power Management Control

The buck–boost converters regulate the power flow to ensure the system runs smoothly and effectively. These are the load power requirements:

$$P_{Loadcalc} = P_{pv} + (P_{Batt} + P_{SC}) \tag{10}$$

where ΔP is the power demand variation.

$$\Delta P = P_{Load} - P_{pv} \tag{11}$$

The system operates as follows: Depending on the state of the power availability requirement between the PV and load, the two storage batteries and SCs can normally operate in either charge or discharge mode. Prolonged power unbalance in the PV-storage system can result in storage deep discharge or overcharging. The PV with batteries/SCs system has three working modes: fully charged mode, normal-charging/discharging of batteries and SCs (normal mode), and transient mode (transient mode).

1-Fully charged mode (FCM):

In this scenario, only two modes appear:M1 and M2.

M1: We disconnected the batteries because they are fully charged.

$$\begin{cases} \Delta P = 0 \\ P_{load} = P_{pv} \\ SOC_{Batt} \geq SOC_{Batt_max} \end{cases} \tag{12}$$

M2: We disconnected the supercapacitors because they are fully charged.

$$\begin{cases} \Delta P = 0 \\ P_{load} = P_{pv} \\ SOC_{SC} \geq SOC_{SC_max} \end{cases} \tag{13}$$

2-Normal mode:

In this scenario, there are two cases. The first one is the charge mode three modes where appear—M4, M5, and M6—where extra power is sent to charge the batteries and SCs. The second case is a discharge mode with only two modes—M3 and M11—where the batteries and supercapacitors are disconnected to protect them as the load is powered by PV power.

a-Charge mode (CM): In this case, we have three modes: M4, M5, and M6.

M4: The generated photovoltaic power supply the load. Excess power is sent to charge the batteries.

$$\begin{cases} \Delta P > 0 \\ P_{load} > P_{pv} \\ SOC_{Batt} < SOC_{Batt_{min}} \\ P_{Batt} = \Delta P = P_{load} - P_{pv} \end{cases} \tag{14}$$

M5: The generated photovoltaic electricity will be used to supply the load. Excess power is used to charge the SCs.

$$\begin{cases} \Delta P > 0 \\ P_{load} > P_{pv} \\ SOC_{SC} < SOC_{SC_min} \\ P_{SC} = \Delta P = P_{load} - P_{pv} \end{cases} \tag{15}$$

M6: PV supplies the load, and any excess power is sent to charge the batteries and supercapacitors.

$$\begin{cases} \Delta P > 0 \\ P_{load} = P_{pv} \\ SOC_{Batt} < SOC_{Batt_min} \\ SOC_{SC} < SOC_{SC_min} \\ P_{Batt} = \Delta P/2 = (P_{load} - P_{pv})/2 \\ P_{SC} = \Delta P/2 = (P_{load} - P_{pv})/2 \end{cases} \quad (16)$$

b-Discharge mode (DM):

M3: When the batteries and supercapacitors are not fully charged, the algorithm acts to prevent the batteries and SCs deep discharging, so disconnecting them is the priority.

$$\begin{cases} \Delta P = 0 \\ P_{load} = P_{pv} \\ SOC_{Batt} < SOC_{Batt_max} \\ SOC_{SC} < SOC_{SC_max} \end{cases} \quad (17)$$

M11: The load could not be supplied by the PV, which can be very low, and we disconnected the batteries and SCs because of their low levels of SOC.

$$\begin{cases} \Delta P < 0 \\ P_{pv} > 0 \\ P_{load} = 0 \\ SOC_{Batt} \leq SOC_{Batt_min} \\ SOC_{SC} \leq SOC_{SC_min} \end{cases} \quad (18)$$

3-Transient mode (TM): We have four modes: M7, M8, M9, M10, and M11.

M7: The batteries are charged; the load is supplied since $SOC_{Batt} > SOC_{Batt_min}$ and the photovoltaic power is zero.

$$\begin{cases} \Delta P < 0 \\ P_{pv} = 0 \\ P_{load} = P_{Batt} \\ SOC_{Batt} > SOC_{Batt_min} \end{cases} \quad (19)$$

M8: As long as the batteries remain charged and the PV power is not null, they will fill up the power gap and supply the load by compensation.

$$\begin{cases} \Delta P < 0 \\ P_{pv} > 0 \\ P_{load} = P_{pv} + P_{Batt} \\ SOC_{Batt} > SOC_{Batt_min} \end{cases} \quad (20)$$

M9: Since there is no PV power in this scenario, charged SCs will be used to feed the load.

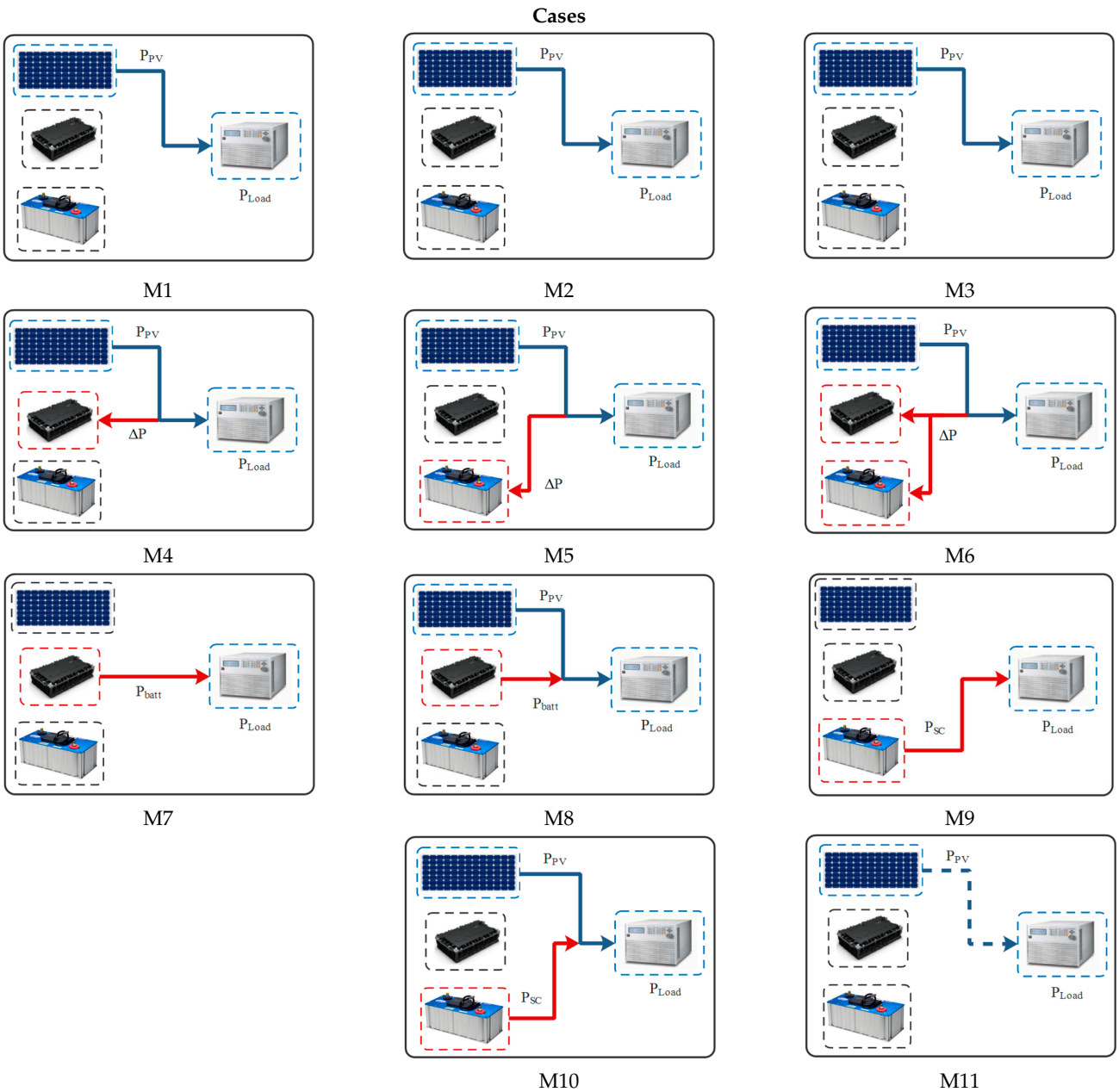
$$\begin{cases} \Delta P < 0 \\ P_{pv} = 0 \\ P_{load} = P_{SC} \\ SOC_{SC} > SOC_{SC_min} \end{cases} \quad (21)$$

M10: Since the $SOC_{SC} > SOC_{SC_min}$, SCs can provide energy, compensating the deficit of photovoltaic power.

$$\begin{cases} \Delta P < 0 \\ P_{pv} > 0 \\ P_{load} = P_{pv} + P_{SC} \\ SOC_{SC} > SOC_{SC_min} \end{cases} \quad (22)$$

When the batteries and supercapacitors are completely charged/discharged, the charging/discharging stops. The eleven possible modes are shown in Table 7. The flowchart (Figure 10) shows how it works.

Table 7. The different possible modes.



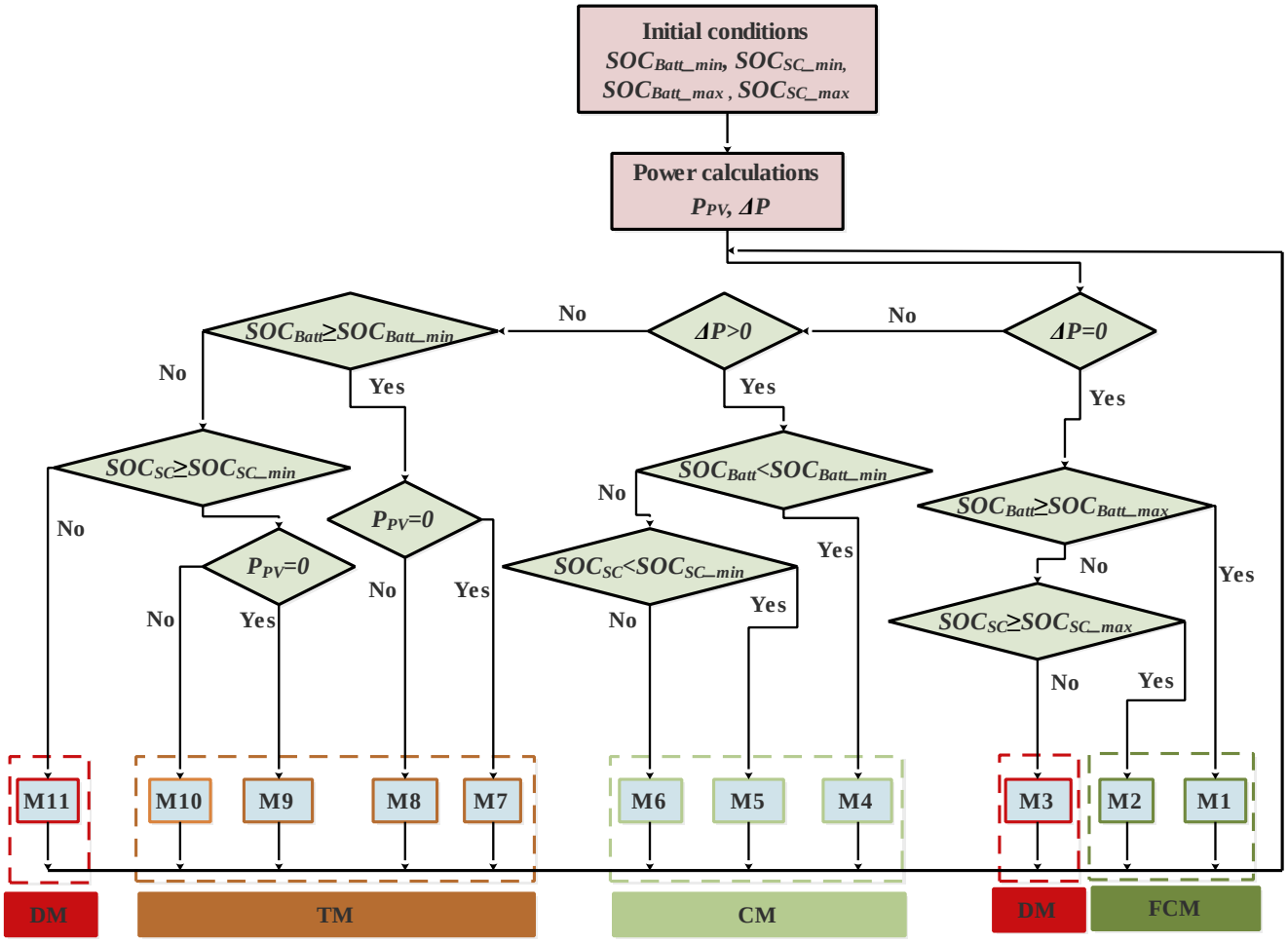
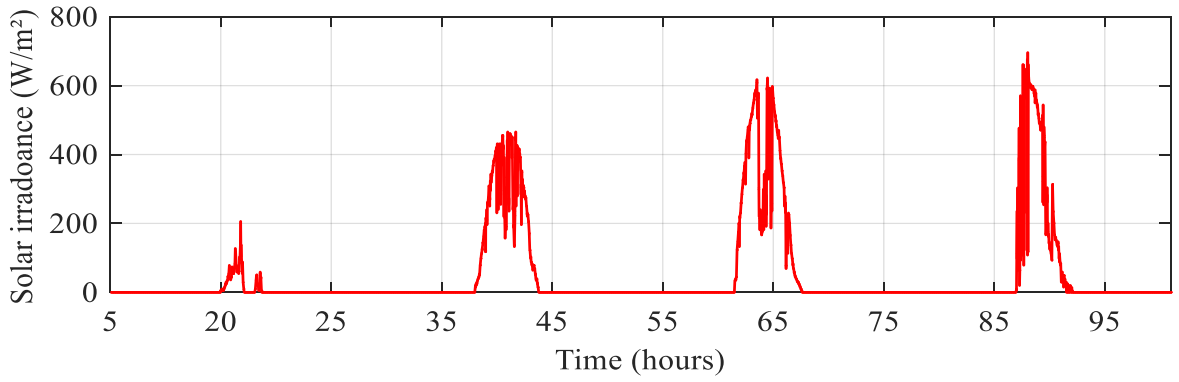


Figure 10. Photovoltaic system energy management flowchart.

6. Simulation Results

The studied system is simulated under MATLAB/Simulink to verify the suggested control and energy management technique. The simulation's findings have been presented and analyzed. The measured profiles of solar irradiation and ambient temperature are given in Figure 11a,b, respectively.



(**a**)

Figure 11. *Cont.*

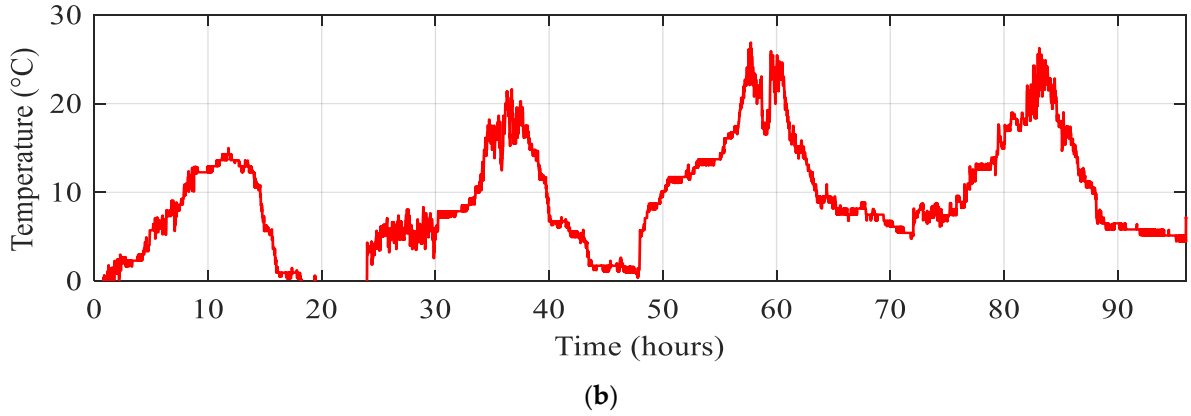


Figure 11. Measured profiles; (**a**) solar irradiance; (**b**) ambient temperature.

DC bus voltage closely tracks its reference (Figure 12). It is regulated in the desired voltage and remains at its reference (V_{DCref} = 24 V), with low fluctuations (ΔV = 0.98% < 1%). Finally, the voltage V_{DCref} meets the load demands with great control efficiency. A well-performing V_{DCref} permits proper operation in the studied system. This result indicates the effectiveness of DC bus voltage regulation that contributes to the optimal operation.

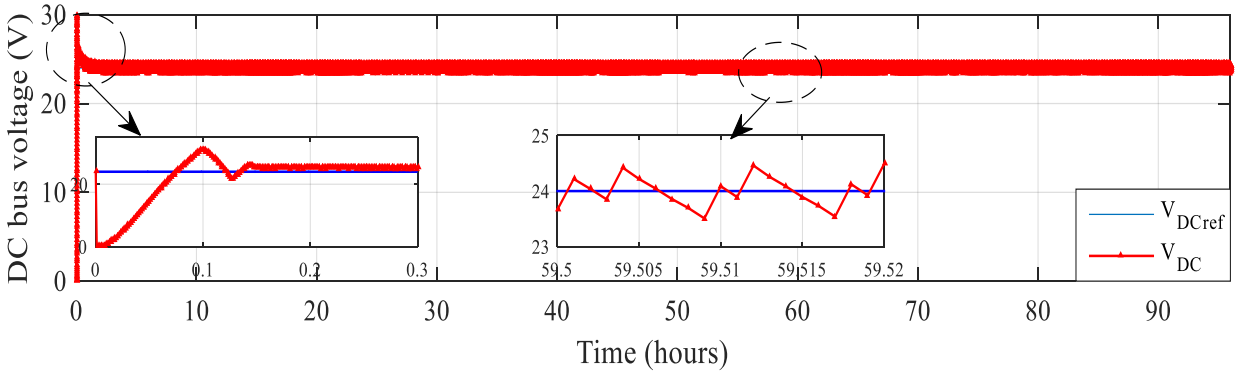


Figure 12. DC bus voltage and its zoom.

Figure 13 presents the simulated voltage profiles of the battery and supercapacitor over time. The batteries and SCs voltage vary in accordance with the power absorbed/injected into the DC bus. Monitoring these voltage profiles is crucial to ensure that the energy storage components are appropriately charged and discharged. Proper voltage control helps maximize the efficiency and lifespan of the energy storage system. By presenting these simulation results and profiles, the study demonstrates the practical application of the proposed control and energy management technique. Analyzing these outcomes allows researchers to evaluate how well the suggested approach performs under varying environmental conditions and dynamic system behavior. It also provides insights into the system's response to different inputs and perturbations, helping validate the efficacy of the strategy.

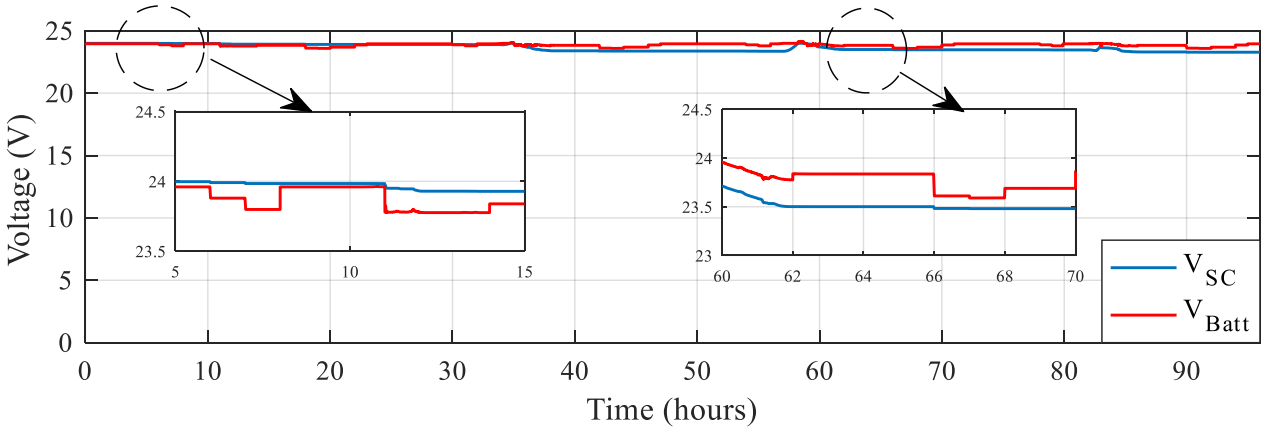


Figure 13. Voltage battery and supercapacitor.

It is noticed in Figure 14 that the battery SOC is well controlled and is maintained between 82.85%and 90% while supercapacitor SOC varies between 58.05% and 90%. The batteries and SCs SOCs are kept within bounds, regardless of the variations in PV and load power profiles.

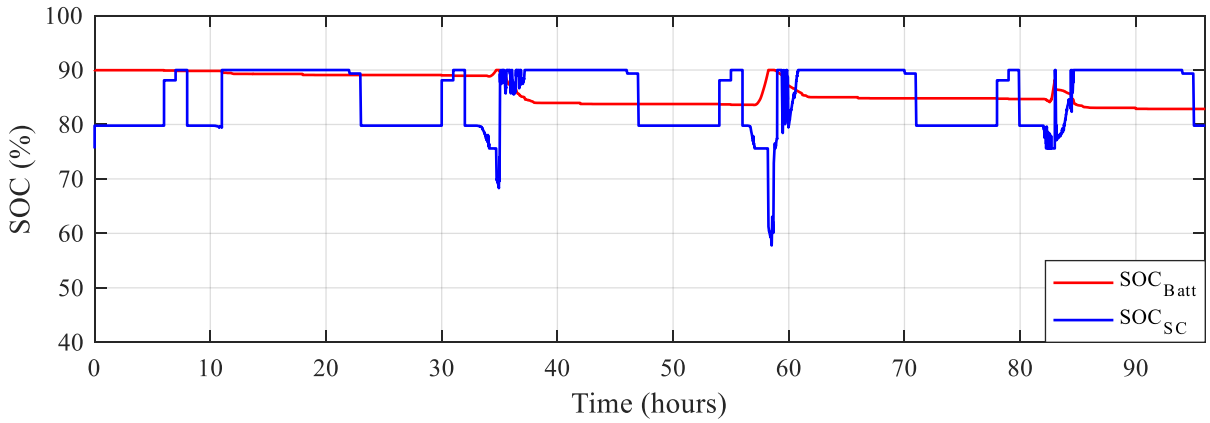


Figure 14. Battery and supercapacitors.

We have conducted a simulation comparing two scenarios: one with only battery storage and another with a hybrid storage system by incorporating both batteries and SCs. Based on our simulation results (specifically shown in Figure 15a,b), we have observed that introducing supercapacitors in the storage system led to a reduction in stress on the batteries. In the scenario with only battery storage, the SOC started at 75% and decreased over time. However, when supercapacitors and a well-implemented control loop were introduced in the system, the battery SOC remained relatively constant and reached a minimum value of 82.85%. It suggests that adding supercapacitors helped regulate the battery SOC and prevent it from dropping significantly. In the battery-only scenario, the battery voltage likely fluctuated as the SOC decreased, which is typical behavior for batteries. The battery voltage remained relatively stable with some fluctuations with the hybrid storage setup including supercapacitors and a control loop. This stability indicates that the supercapacitors might be assisting in maintaining a steady voltage level, contributing to more consistent system performance.

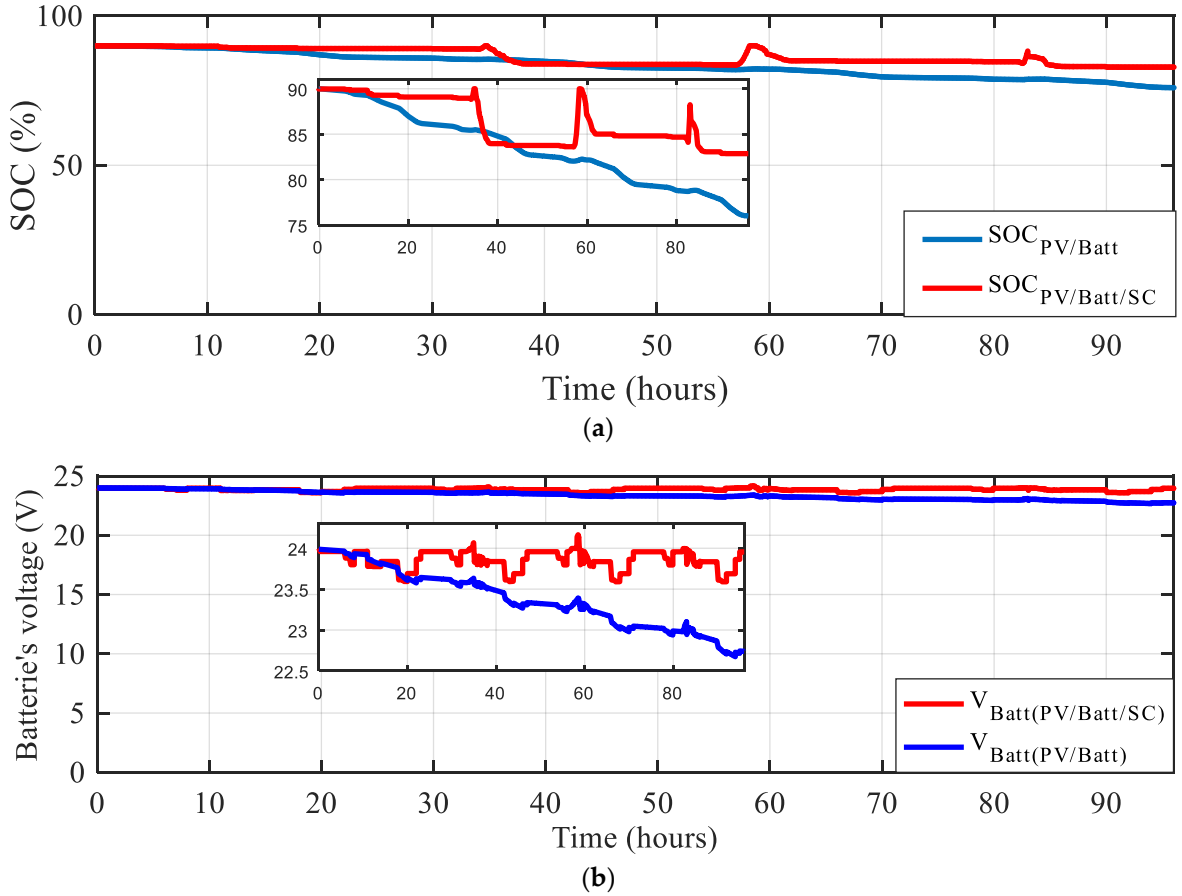


Figure 15. Battery SOC and voltage with and without introduction of supercapacitors. (**a**) Battery SOC. (**b**) Voltage battery.

Figure 16 shown below points out the battery and supercapacitor currents.

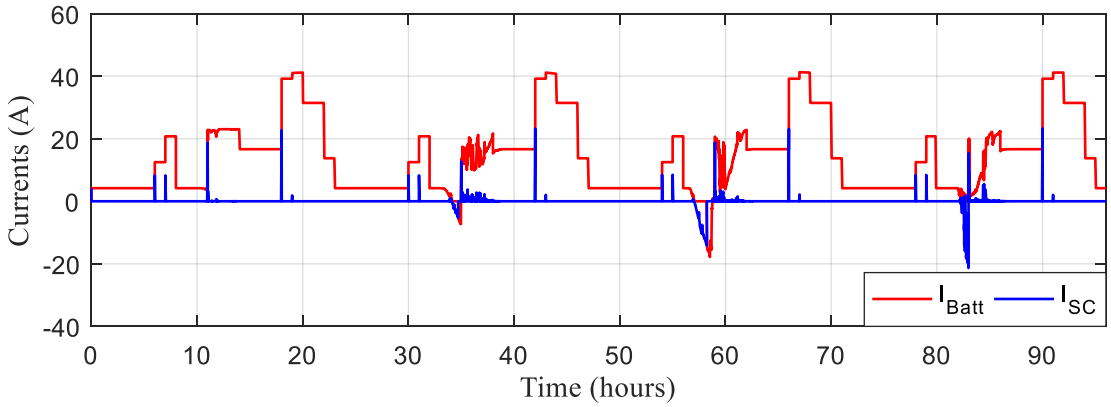


Figure 16. Battery and supercapacitor currents.

The different resulting modes are given in Figure 17. During each cycle, batteries and SCs are discharged and then rapidly recharged at M4 and M6 modes (for batteries and at M5 and M6 for SCs). The only cases of disconnection are during M3 where $\Delta P = 0$ but the load is powered entirely by photovoltaics, and during M11 where the load is disconnected.

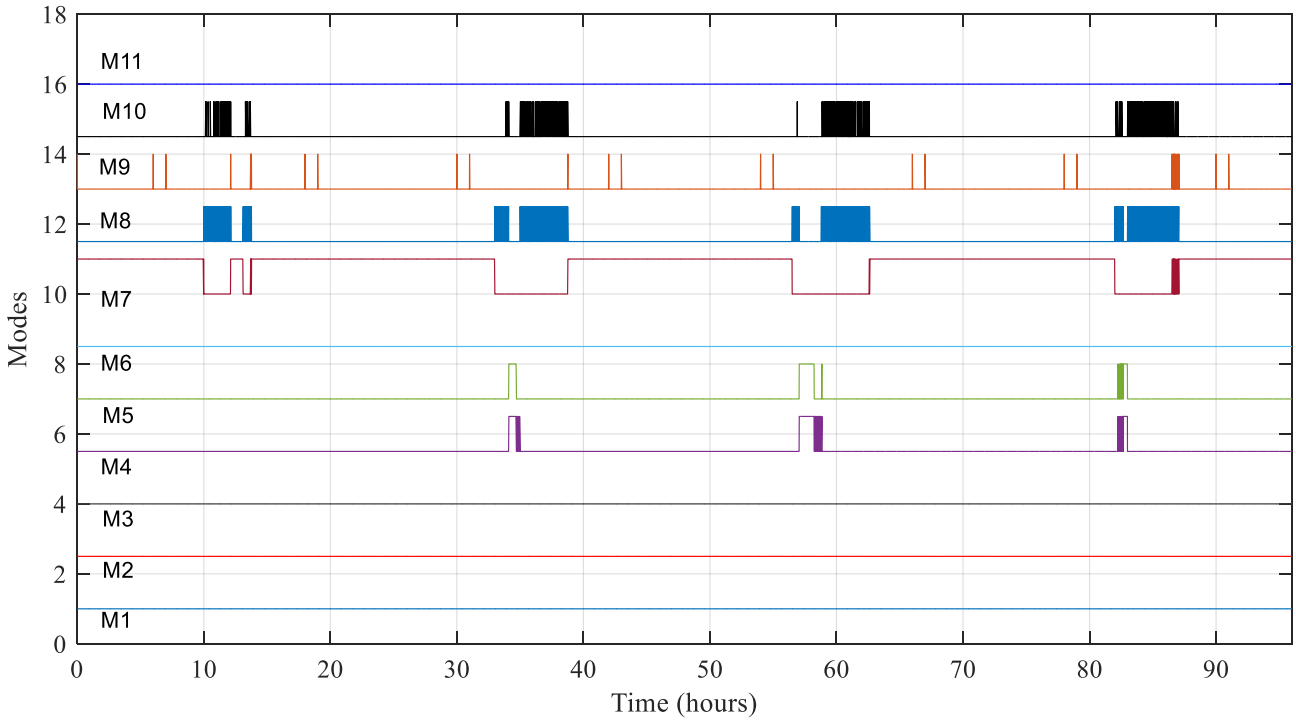


Figure 17. Different obtained modes.

Figure 18 depicts the battery, supercapacitor, and PV powers all at once.

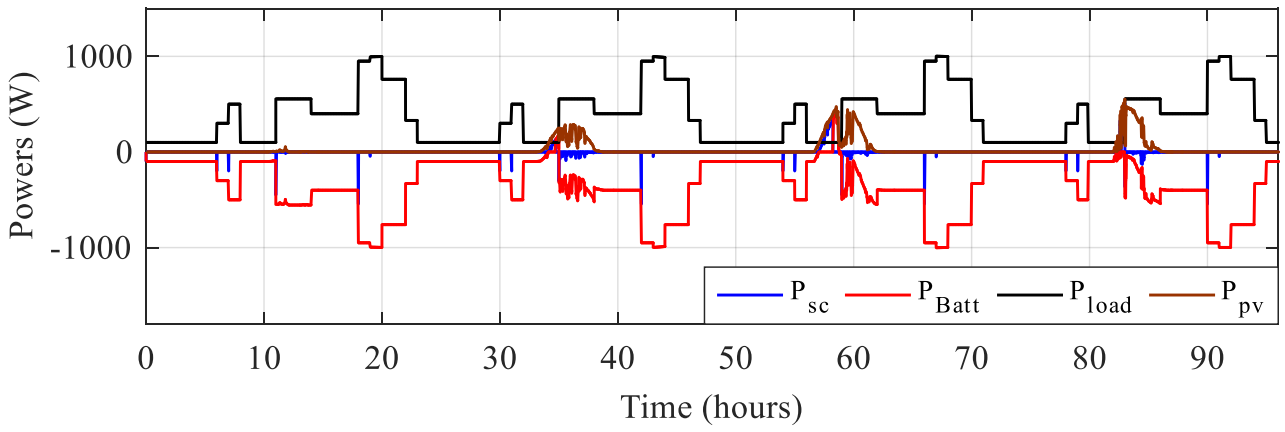


Figure 18. The different powers.

Figure 19 depicts the power per day of all power sources for four distinct days. The PV power varies with the profile of solar irradiation. Despite changes in load requirements, the curve of maximum available PV power aligns with solar irradiance variation, validating the suggested MPPT. To better depict discharges in relation to PV and load changes, battery and SC powers are presented in negative. It should be noted that the negative sign of the batteries' and SCs' powers indicates that they are recovering power, while the positive sign indicates that they are supplying the load. They alter its charging course (sign).

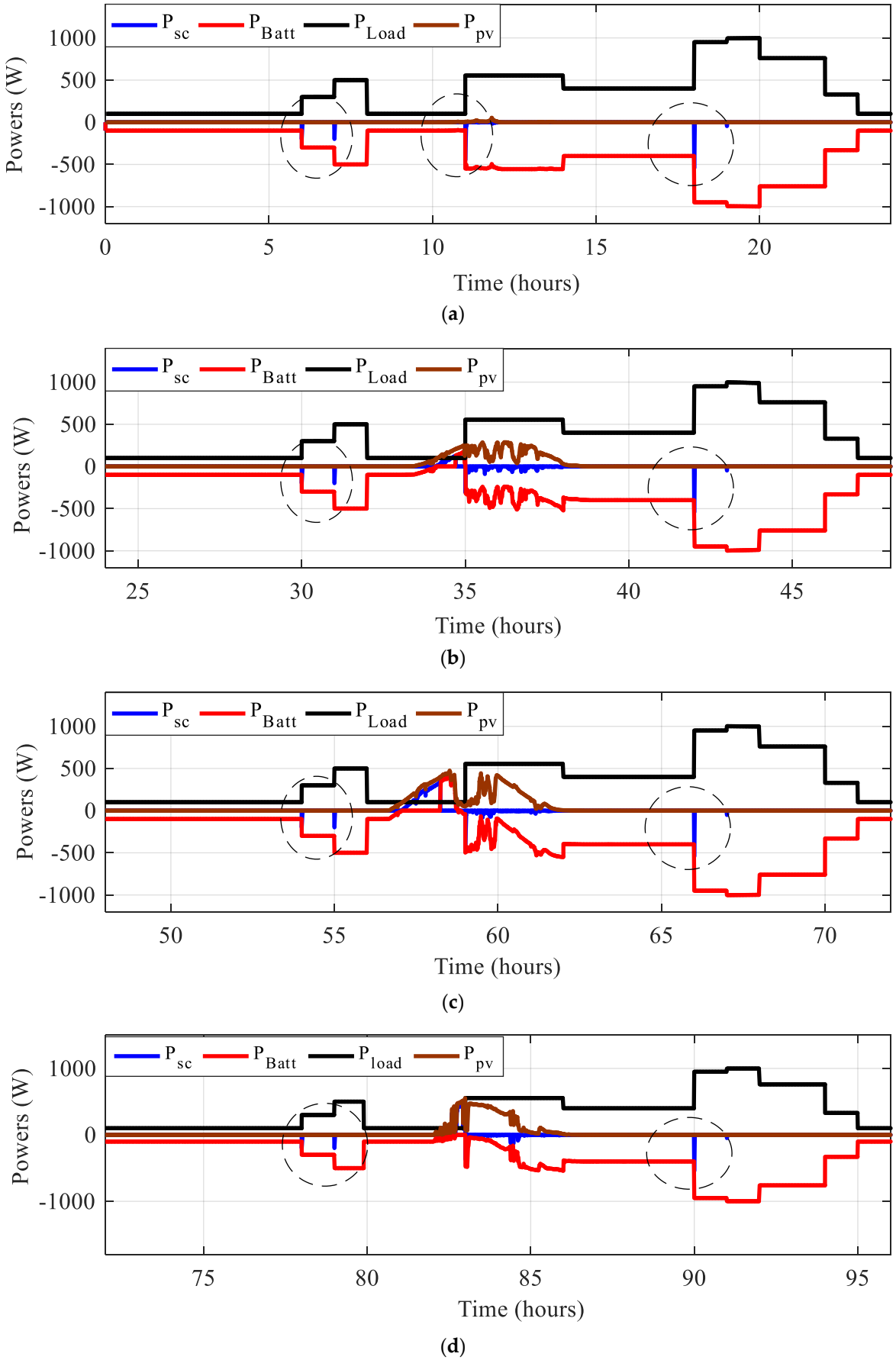


Figure 19. Powers per day with the different modes. (**a**) Day 1. (**b**) Day 2. (**c**) Day 3. (**d**) Day 4.

During the first day (Figure 19a), where solar irradiance is very low and does not exceed 200 W/m^2, the battery is highly stressed and is supported by the SC during sudden changes in load (at t = 6, 7, 11, and 18 h). The most frequent modes are M7, M8, M9, and M10, as ΔP is always negative. On the second day (Figure 19b), when maximum solar irradiation is around 460 W/m^2, the same observations were made, with slightly less stress on the batteries, assisted by the SC, at times of abrupt load changes (t = 31 and 41 h). On the third day (Figure 19c), solar irradiance reached 620 W/m^2, and up to 740 W/m^2 on the fourth day. On these last two days, we note less stress on the batteries and the presence of modes M4 and M5, corresponding to battery and SC charging.

The reference load power and the sum of power developed by all the power sources are shown in Figure 20, respectively.

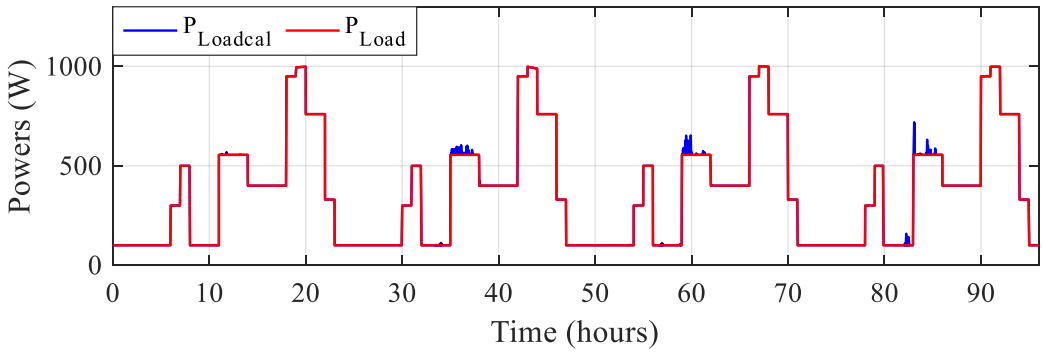


Figure 20. Calculated $P_{Load-cal}$ and developed load power P_{Load}.

The zoom of this last-mentioned figure for four distinct days is shown in Figure 21.

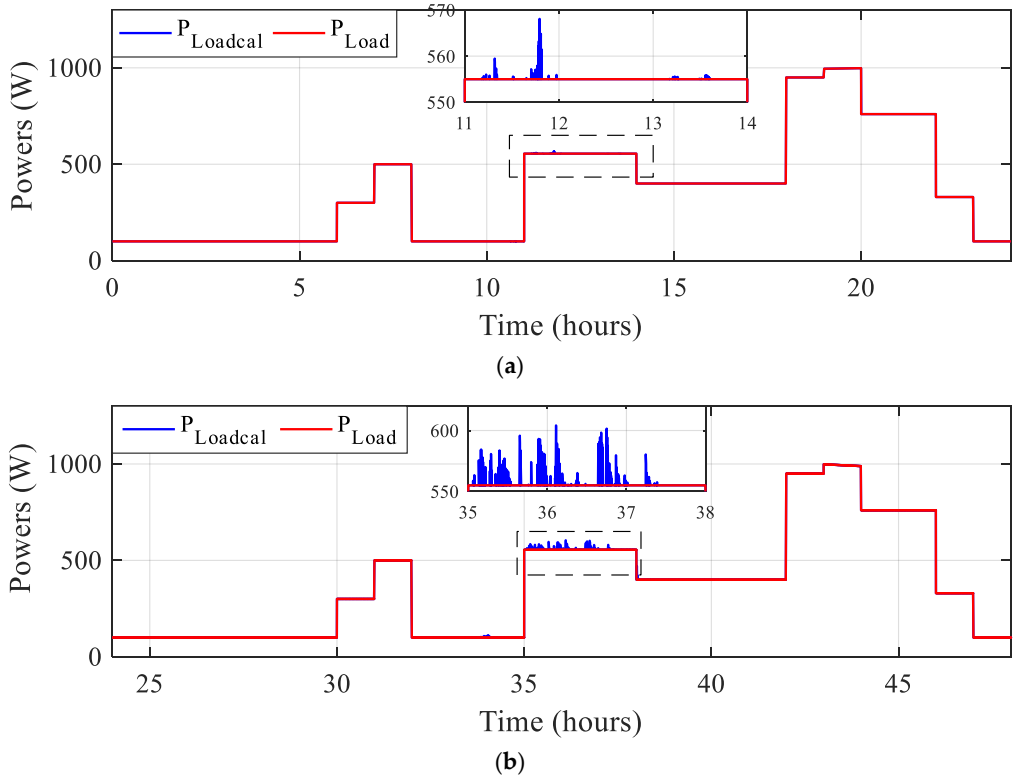


Figure 21. *Cont.*

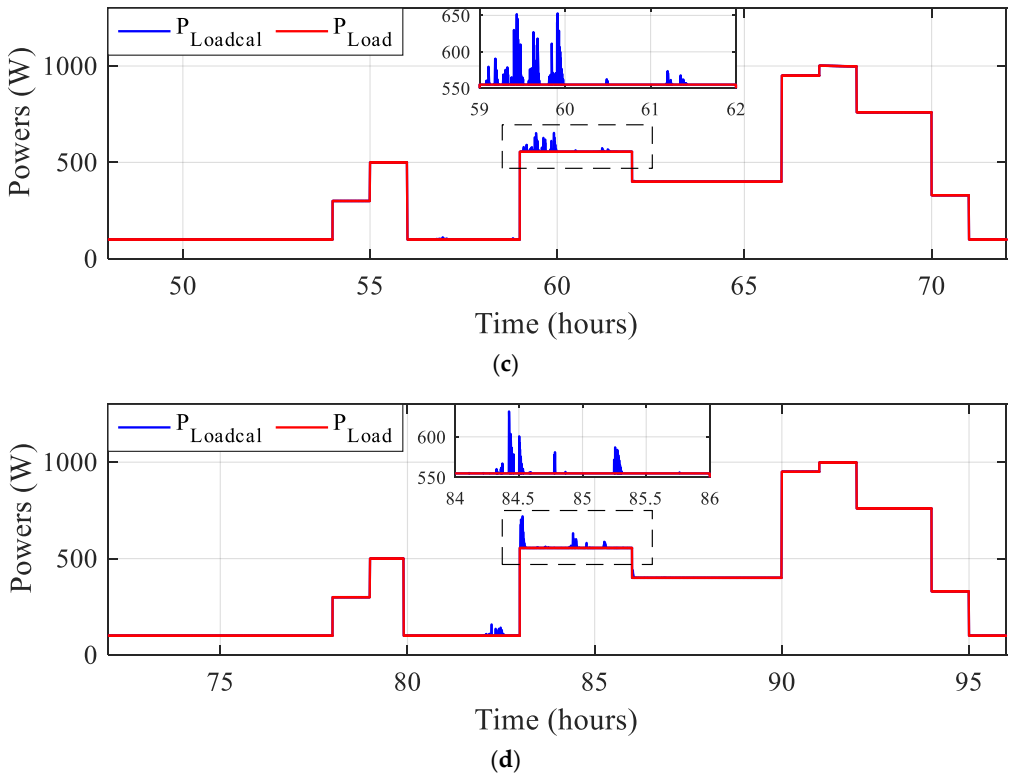


Figure 21. Zooms on calculated and developed load power. (**a**) Day 1. (**b**) Day 2. (**c**) Day 3. (**d**) Day 4.

Sometimes the calculated power is more than the developed load power. The power surplus has been computed (Figure 21). Despite adequate size and the use of PMC, it is noted that a slight surplus of power is obtained, which can reach a maximum of 100 W on the last day of strong sun irradiation. They demonstrate the suggested control and energy management technique's performance with regard to state of charge, current profiles, operating modes, power output and consumption, and load needs alignment. These visual representations provide insights into the system's behavior under various settings and indicate the research approach's feasibility and practicality.

7. Real-Time Simulation

A series of experimental tests were performed on a real-time simulator (RT-LAB) to evaluate the proposed control methods. The system settings remained unchanged from the MATLAB/Simulink numerical simulation. The real-time simulation bench (Figure 22) consists of a host PC, a real-time digital simulator (OP5700), an HIL controller, an OP8660 data collection interface, and a digital oscilloscope. Maintaining system parameter consistency, employing particular hardware components, and displaying the experimental bench using a given diagram (Figure 22) were all part of the setup. These real-time experiments validate the proposed control strategies in a practical environment, adding a layer of real-world verification to the findings of the simulation-based study.

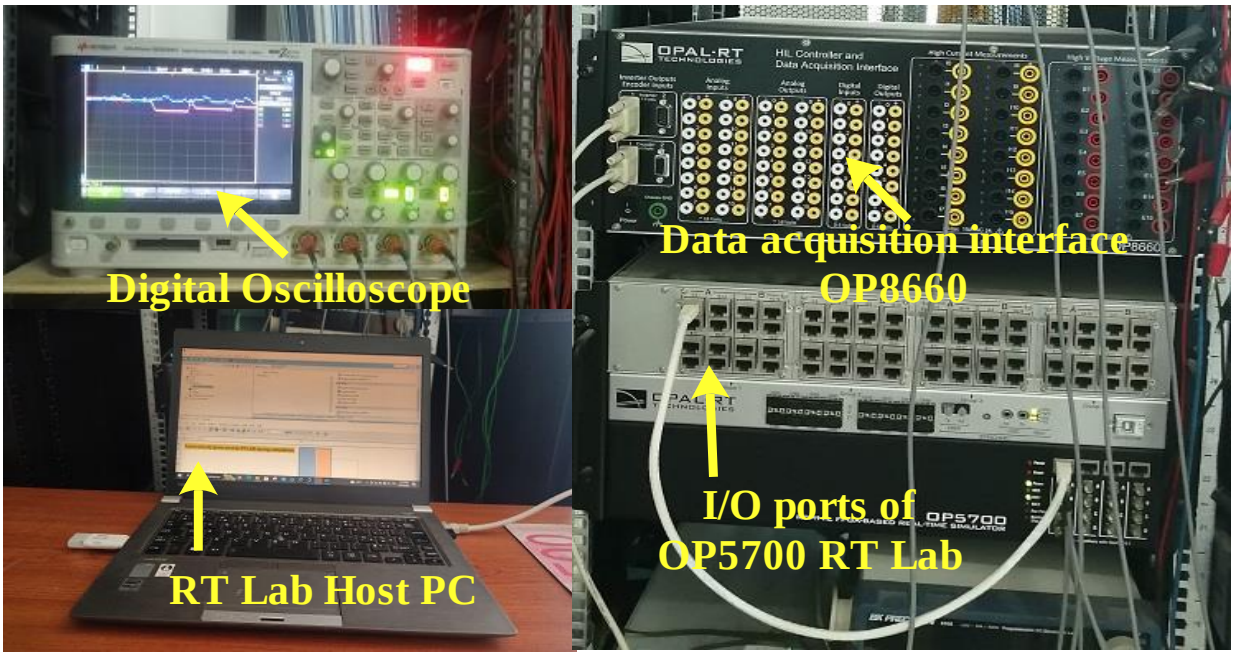


Figure 22. RT-LAB real-time simulator work bench.

Figure 23 shows the different obtained modes when the energy management strategy is run using the RT-LAB real-time simulation platform. The scheduled modes from 1 to 11 are highlighted to demonstrate the efficacy of the suggested management.

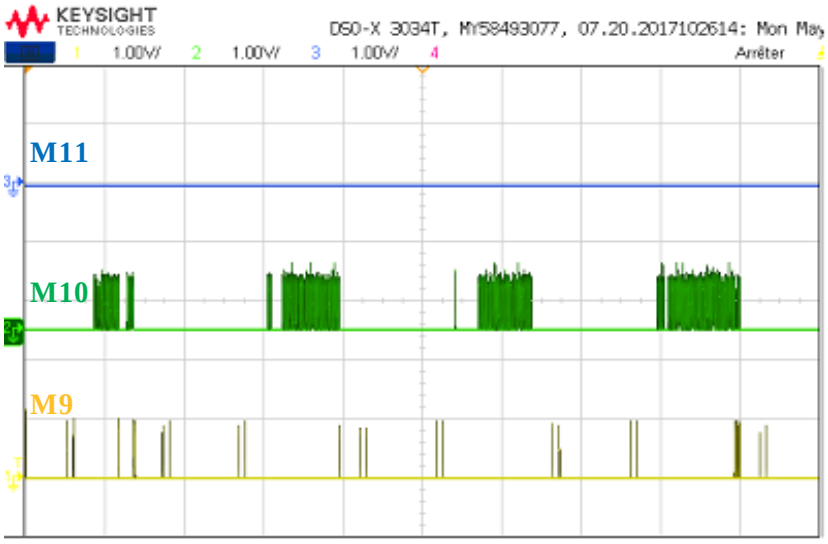


Figure 23. *Cont.*



Figure 23. Different modes obtained in RT-LAB.

Battery and supercapacitor voltages and their corresponding zooms are highlighted in Figure 24.

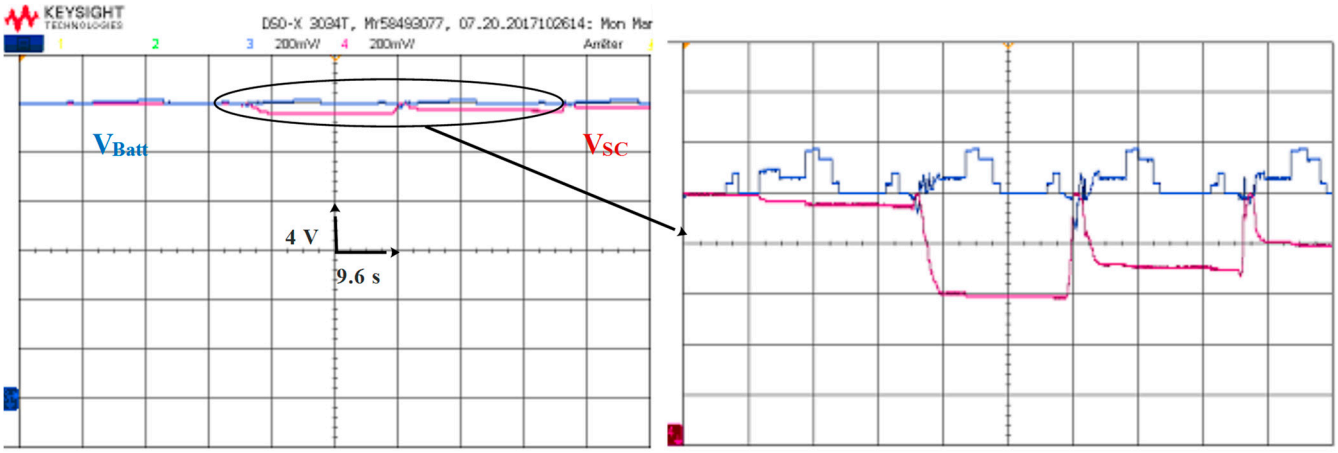


Figure 24. Battery voltage.

The SOC of both the supercapacitor and the battery are shown in Figure 25. The zoom in the same figure confirms that the SOC of the previously mentioned power sources is kept within safe limits during all the simulation periods.

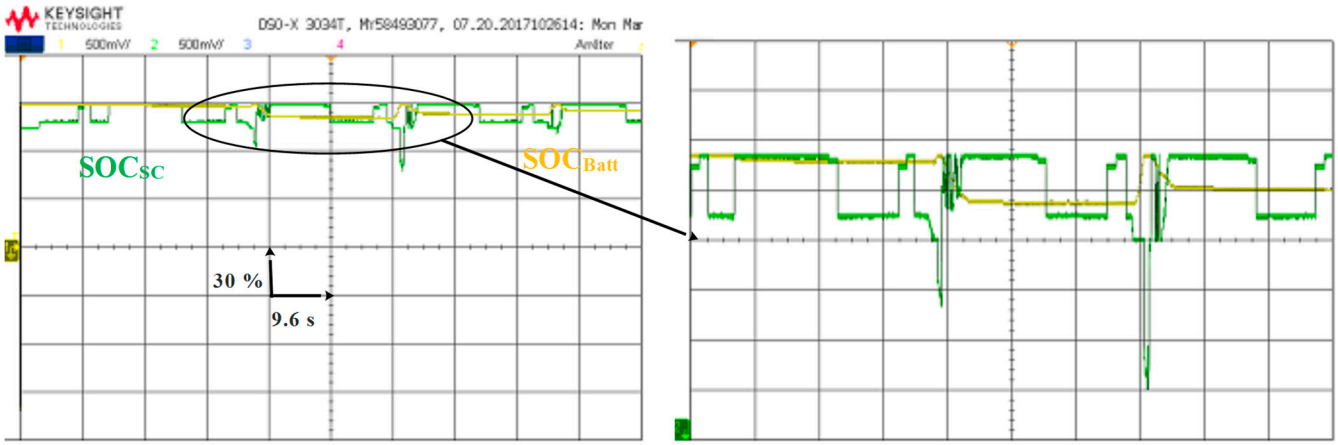


Figure 25. Battery–supercapacitor SOC and their zoom.

Figures 24 and 25, along with their corresponding zooms, provide detailed insights into the behavior of the battery and supercapacitor within the energy management system. It highlights voltage profiles, SOC behavior, and their alignment with safe operating limits, reinforcing the successful performance of the suggested energy management strategy in maintaining optimal conditions for the energy storage components.

The battery and supercapacitor currents are represented in Figure 26. It is noticed that the battery is used during low and medium power demands. However, during fast and peak load demands, the supercapacitor is used because of its rapid transient dynamics.

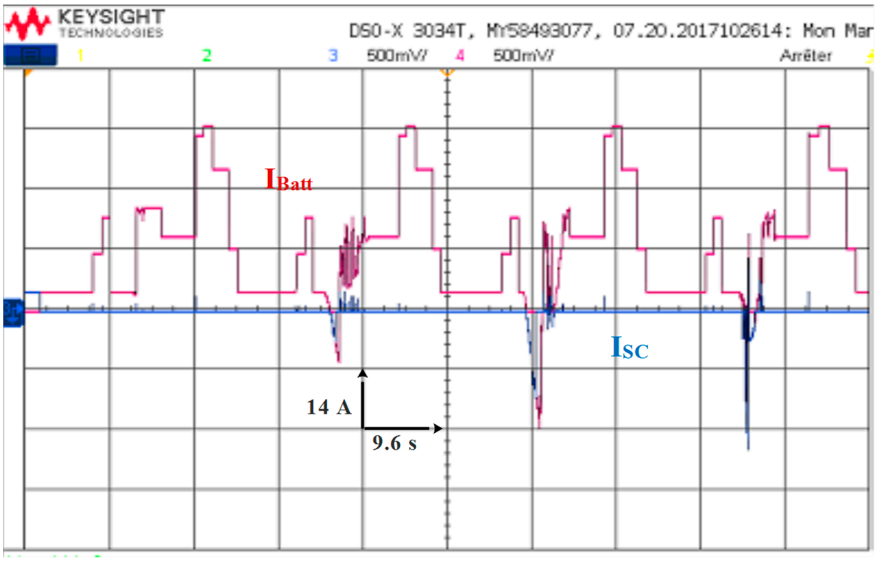


Figure 26. Battery-supercapacitor currents.

Figure 27 shows the reference DC bus voltage, its reference, and a zoom of the aforementioned quantity. It can be seen clearly that V_{DC} precisely follows its reference. Note also that the voltage ripple band is small and tolerable.

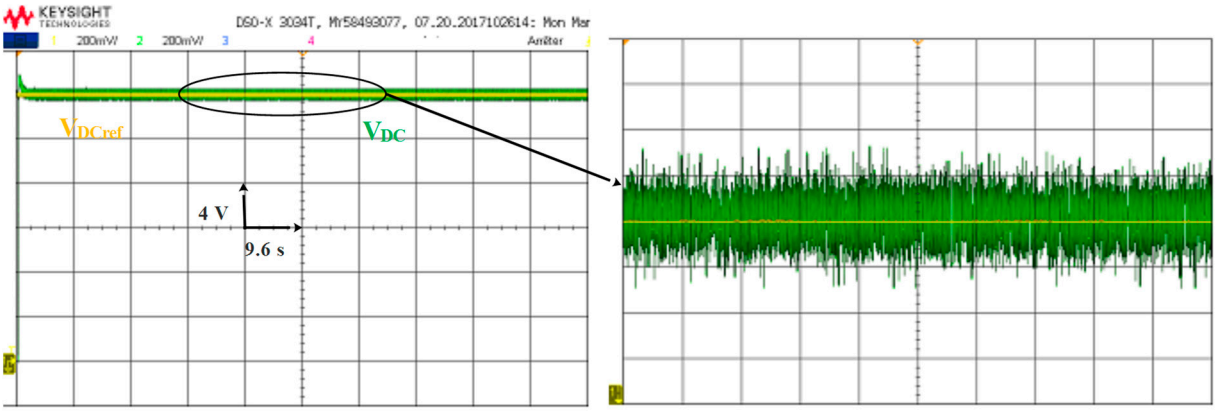


Figure 27. DC bus voltage and its zoom using RT LAB.

The power developed by each energy source is shown separately in Figure 28. As shown in Figure 29, the load power equals the developed power.

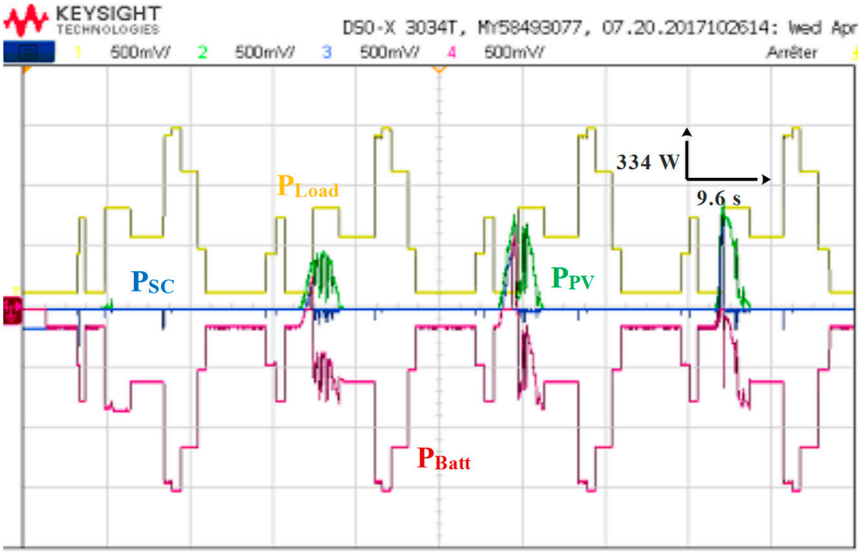


Figure 28. Different energy sources' powers.

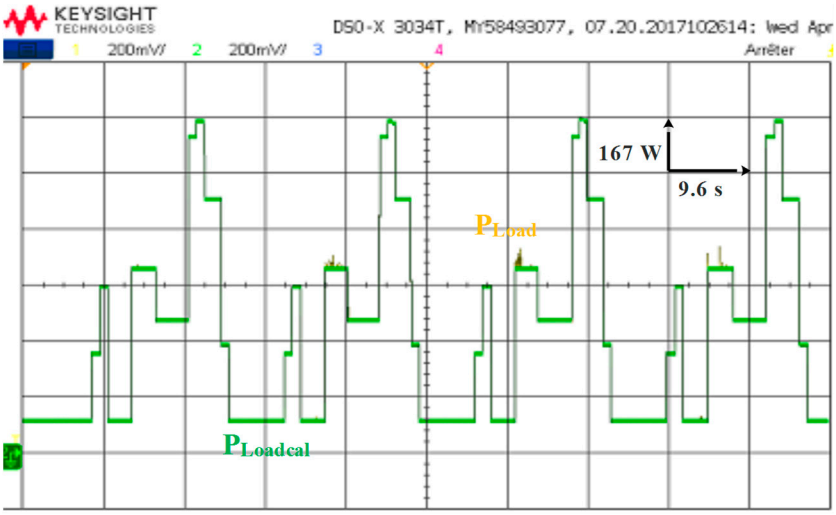


Figure 29. Total developed power P_{Load} and calculated one $P_{Loadcal}$.

One can notice that the storage system produces a power that is equivalent to the total demand with a little excess as illustrated in the different subfigures of Figure 30a–d illustrated below:

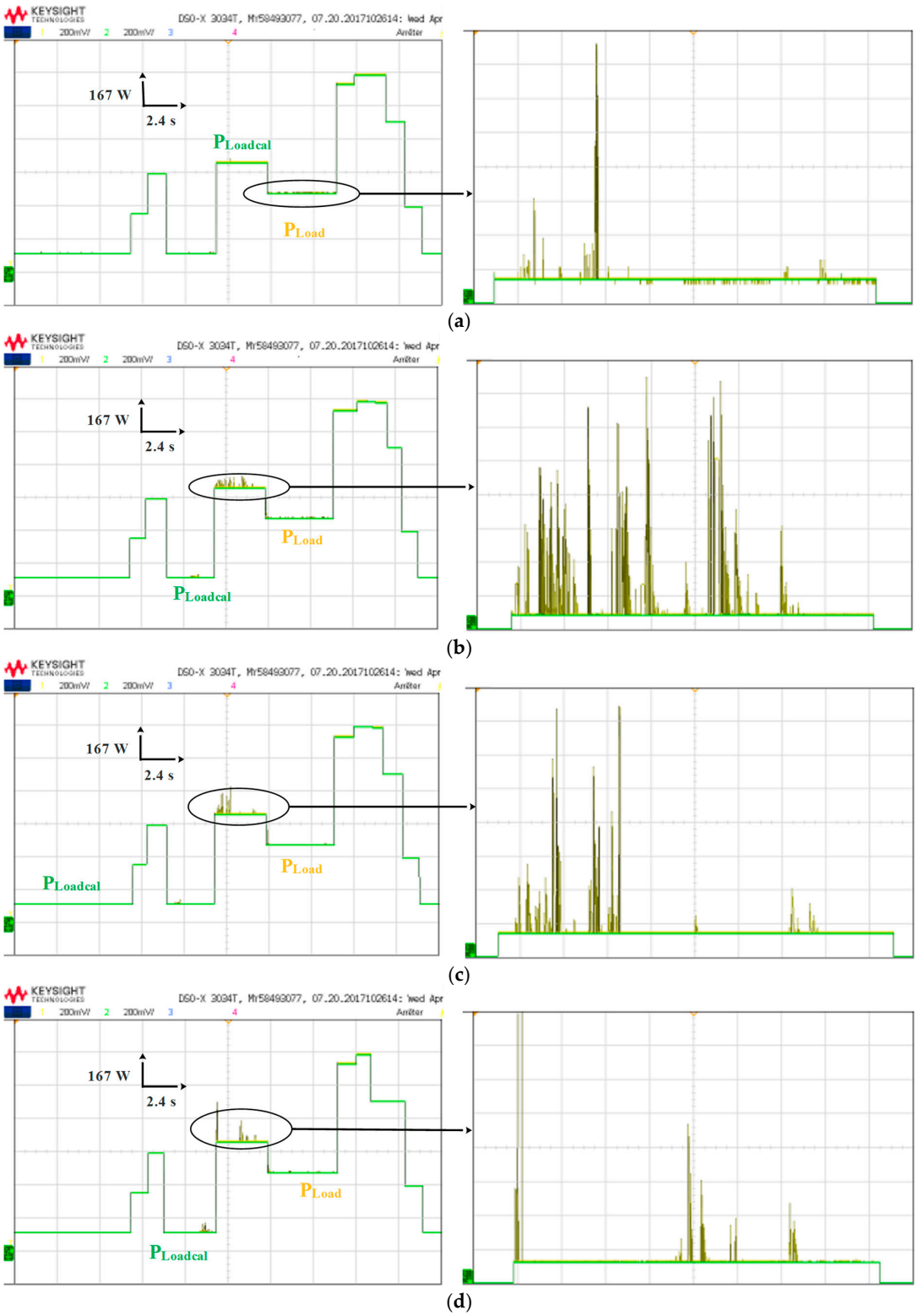


Figure 30. Zooms on calculated and developed load power in RT-LAB. (**a**) Day 1. (**b**) Day 2. (**c**) Day 3. (**d**) Day 4.

8. Conclusions

This paper proposes an energy management strategy for multi-storage (battery/SC) applied in a PV system. The used control technique is based on current regulation of two energy sources through the use of proportional integral (PI) regulators. The findings were verified by simulation with MATLAB/Simulink, and they were also tested in real-time with the RT-LAB simulation platform. This means that the control used is efficient and allows the flow of energy appropriately, ensuring good and optimal system operation. The power management techniques covered in this paper enable the system to operate as effectively as possible with high PV system performance, regardless of the weather conditions. As a further study, it is planned to apply intelligent control methods to extend the lifespan of energy sources while ensuring their efficient and optimal utilization. The authors plan to extend their work by exploring the application of the proposed system in real-world applications such as water pumping in irrigation systems.

Author Contributions: Conceptualization, K.K., A.B. and A.O.; Methodology, D.R., Z.M., T.R., A.A., E.A., A.H.K.A. and S.A.M.A.; Software, D.R., K.K., A.B., Z.M., A.O., T.R., A.A., A.H.K.A. and S.A.M.A.; Validation, D.R., A.B., A.O., T.R., A.A., E.A., A.H.K.A. and S.A.M.A.; Formal analysis, K.K., A.B., Z.M., A.O., T.R., A.A., E.A. and A.H.K.A.; Investigation, D.R., K.K., A.B., Z.M., A.O., T.R., A.A., A.H.K.A. and S.A.M.A.; Resources, D.R., K.K., A.B., Z.M., A.O., T.R., A.A., A.H.K.A. and S.A.M.A.; Data curation, K.K. and A.O.; Writing—original draft, D.R., K.K., A.B., Z.M., A.O., T.R., E.A., A.H.K.A. and S.A.M.A.; Writing—review & editing, D.R., K.K., A.B., A.O., E.A., A.H.K.A. and S.A.M.A.; Funding acquisition, A.B. All authors have read and agreed to the published version of the manuscript.

Funding: This work is funded by the Deanship of Scientific Research, Taif University.

Acknowledgments: The researchers would like to acknowledge the Deanship of Scientific Research, Taif University for funding this work.

Conflicts of Interest: The authors declare no conflict of interest.

References

1. Poshnath, A.; Rismanchi, B.; Rajabifard, A. Adoption of Renewable Energy Systems in Common Properties of Multi-Owned Buildings: Introduction of 'Energy Entitlement'. *Energy Policy* **2023**, *174*, 113465. [CrossRef]
2. Kamarzaman, N.A.; Tan, C.W. A Comprehensive Review of Maximum Power Point Tracking Algorithms for Photovoltaic Systems. *Renew. Sustain. Energy Rev.* **2014**, *37*, 585–598. [CrossRef]
3. Elgendy, J.-M.A.; Zahawi, B.; Atkinson, D.J. Assessment of Perturb and Observe MPPT Algorithm Implementation Techniques for PV Pumping Applications. *IEEE Trans. Sustain. Energy* **2012**, *3*, 21–33. [CrossRef]
4. Sahoo, S.; Timmann, P. Energy Storage Technologies for Modern Power Systems: A Detailed Analysis of Functionalities, Potentials, and Impacts. *IEEE Access* **2023**, *11*, 49689–49729. [CrossRef]
5. Attia, H. Fuzzy Logic Controller Effectiveness Evaluation through Comparative Memberships for Photovoltaic Maximum Power Point Tracking Function. *Int. J. Power Electron. Drive Syst.* **2018**, *9*, 1147–1156. [CrossRef]
6. Liu, J.; Yang, M.; Wang, T. Impedance-Based Stability Analysis of Grid-Tied Photovoltaic System with Superconducting Magnetic Energy Storage System. *IEEE Trans. Appl. Supercond.* **2021**, *31*, 5402504. [CrossRef]
7. Kumar, R.N. Energy Management System for Hybrid RES with Hybrid Cascaded Multilevel Inverter. *Int. J. Electr. Comput. Eng.* **2014**, *4*, 24–30. [CrossRef]
8. Dursun, E.; Kilic, O. Comparative Evaluation of Different Power Management Strategies of a Stand-Alone PV/Wind/PEMFC Hybrid Power System. *Electr. Power Energy Syst.* **2012**, *34*, 81–89. [CrossRef]
9. Bratcu, A.I.; Munteanu, I.; Bacha, S.; Raison, B. Maximum Power Point Tracking of Grid-Connected Photovoltaic Arrays by Using Extremum Seeking Control. *J. Control Eng. Appl. Inform.* **2008**, *10*, 3–12.
10. Shafique, M.; Akbar, A.; Rafiq, M.; Azam, A.; Luo, X. Global Material Flow Analysis of End-of-Life of Lithium Nickel Manganese Cobalt Oxide Batteries from Battery Electric Vehicles. *Waste Manag. Res.* **2023**, *41*, 376–388. [CrossRef]
11. Singh, S.N.; Snehlata, N. Intelligent Home Energy Management by Fuzzy Adaptive Control Model for Solar (PV)-Grid/DG Power System in India. *Int. J. Power Control Signal Comput.* **2011**, *2*, 61–66.
12. Hajizadeh, A.; Golkar, M.A. Intelligent Power Management Strategy of Hybrid Distributed Generation System. *Electr. Power Energy Syst.* **2007**, *29*, 783–795. [CrossRef]
13. Zhou, X.; Liu, Q.; Ma, Y.; Xie, B. DC-Link Voltage Research of Photovoltaic Grid-Connected Inverter Using Improved Active Disturbance Rejection Control. *IEEE Access* **2021**, *9*, 9884–9894. [CrossRef]

14. Sumarmad, K.A.A.; Sulaiman, N.; Wahab, N.I.A.; Hizam, H. Microgrid Energy Management System Based on Fuzzy Logic and Monitoring Platform for Data Analysis. *Energies* **2022**, *15*, 4125. [CrossRef]
15. Zhang, X.; Zhan, L.; Qi, L. Performance Enhancement Method for Power Electronic Switch in Hybrid DC Circuit Breaker Based on Partial Precooling. *IEEE Trans. Power Electron.* **2023**, *38*, 118–122. [CrossRef]
16. Soulatiantork, P. Performance Comparison of a Two PV Module Experimental Setup Using a Modified MPPT Algorithm under Real Outdoor Conditions. *Sol. Energy* **2018**, *169*, 401–410. [CrossRef]
17. Farag, M.M.; Patel, N.; Hamid, A.K.; Adam, A.A.; Bansal, R.C.; Bettayeb, M.; Mehiri, A. An Optimized Fractional Nonlinear Synergic Controller for Maximum Power Point Tracking of Photovoltaic Array under Abrupt Irradiance Change. *IEEE J. Photovolt.* **2023**, *13*, 305–314. [CrossRef]
18. Smida, M.B.; Sakly, A. Fuzzy Logic Control of a Hybrid Renewable Energy System: A Comparative Study. *Wind Eng.* **2021**, *45*, 793–806. [CrossRef]
19. Haseeb, A.; Waleed, U.; Ashraf, M.M.; Siddiq, F.; Rafiq, M.V.; Shafique, M. Hybrid Weighted Least Square Multi-Verse Optimizer (WLS–MVO) Framework for Real-Time Estimation of Harmonics in Non-Linear Loads. *Energies* **2023**, *16*, 609. [CrossRef]
20. Khan, M.A.; Zeb, K.; Sathishkumar, P.; Ali, M.U.; Uddin, W.; Hussain, S.; Ishfaq, M.; Khan, I.; Cho, H.-G.; Kim, H.-J. A Novel Supercapacitor/Lithium-Ion Hybrid Energy System with a Fuzzy Logic-Controlled Fast Charging and Intelligent Energy Management System. *Electronics* **2018**, *7*, 63. [CrossRef]
21. Glavin, M.E.; Hurley, W.G. Optimizations of a photovoltaic battery ultracapacitor hybrid energy storage system. *Sol. Energy* **2012**, *86*, 3009–3020. [CrossRef]
22. Jing, W.L.; Lai, C.H.; Wong, W.S.; Wong, M.D. Cost analysis of battery-supercapacitor hybrid energy storage system for standalone PV systems. In Proceedings of the 4th IET Clean Energy and Technology Conference, Kuala Lumpur, Malaysia, 14–15 November 2016. [CrossRef]
23. Shrivastava, A.; Gupta, S. Review on Super Capacitor-Battery based Hybrid Energy Storage System for PV Application. *Int. J. Adv. Eng. Manag. Sci.* **2017**, *3*, 378–381. [CrossRef]
24. Logerais, P.O.; Riou, O.; Camara, M.A.; Durastanti, J.F. Study of photovoltaic energy storage by supercapacitors through both experimental and modeling approaches. *J. Sol. Energy* **2013**, *2013*, 659014. [CrossRef]
25. Uzunoglu, M.; Alam, M.S. Dynamic modeling, design, and simulation of a combined PEM fuel cell and ultracapacitor system for stand-alone residential applications. *IEEE Trans. Energy Convers.* **2006**, *21*, 767–775. [CrossRef]
26. Thounthong, P.; Pierfederici, S.; Martin, J.P.; Hinaje, M.; Davat, B. Modeling and control of fuel cell/supercapacitor hybrid source based on differential flatness control. *IEEE Trans. Veh. Technol.* **2010**, *59*, 2700–2710. [CrossRef]
27. Glavin, M.E.; Chan, P.K.; Armstrong, S.; Hurley, W.G. A stand-alone photovoltaic supercapacitor battery hybrid energy storage system. In Proceedings of the 2008 13th International Power Electronics and Motion Control Conference, Poznan, Poland, 1–3 September 2008; pp. 1688–1695. [CrossRef]
28. Guerra, M.I.S.; de Araujo, F.M.U.; Dhimish, M.; Vieira, R.G. Assessing Maximum Power Point Tracking Intelligent Techniques on a PV System with a Buck–Boost Converter. *Energies* **2021**, *14*, 7453. [CrossRef]
29. Reddy, R.M.; Das, M.; Chauhan, N. Novel Battery-Supercapacitor Hybrid Energy Storage System for Wide Ambient Temperature Electric Vehicles Operation. *IEEE Trans. Circuits Syst. II Express Briefs* **2023**, *70*, 2580–2584. [CrossRef]
30. Jia, C.; Cui, J.; Qiao, W.; Qu, L. Real-Time Model Predictive Control for Battery-Supercapacitor Hybrid Energy Storage Systems Using Linear Parameter-Varying Models. *IEEE J. Emerg. Sel. Top. Power Electron.* **2023**, *11*, 251–263. [CrossRef]
31. Nguyen, N.-D.; Yoon, C.; Lee, Y.I. A Standalone Energy Management System of Battery/Supercapacitor Hybrid Energy Storage System for Electric Vehicles Using Model Predictive Control. *IEEE Trans. Ind. Electron.* **2023**, *70*, 5104–5114. [CrossRef]
32. Roy, P.; Liao, Y.; He, J. Economic Dispatch for Grid-Connected Wind Power with Battery-Supercapacitor Hybrid Energy Storage System. *IEEE Trans. Ind. Appl.* **2023**, *59*, 1118–1128. [CrossRef]
33. Belaid, S.; Rekioua, D.; Oubelaid, A.; Ziane, D.; Rekioua, T. Proposed Hybrid Power Optimization for Wind Turbine/Battery System. *Period. Polytech. Electr. Eng. Comput. Sci.* **2022**, *66*, 60–71. [CrossRef]
34. Pourmousavi, S.A.; Nehrir, M.H.; Colson, C.M.; Wang, C. Real-time energy management of a stand-alone hybrid wind-microturbine energy system using particle swarm optimization. *IEEE Trans. Sustain. Energy* **2010**, *1*, 193–201. [CrossRef]
35. Oubelaid, A.; Taib, N.; Rekioua, T. Novel coordinated power sources switching strategy for transient performance enhancement of hybrid electric vehicles. *COMPEL Int. J. Comput. Math. Electr. Electron. Eng.* **2022**, *41*, 1880–1919. [CrossRef]
36. Elmorshe, M.F.; Elkadeem, M.R.; Kotb, K.M.; Taha, I.B.M.; Mazzeo, D. Optimal design and energy management of an isolated fully renewable energy system integrating batteries and supercapacitors. *Energy Convers. Manag.* **2021**, *245*, 114584. [CrossRef]
37. Azuara-Grande, L.S.; Arnaltes, S.; Alonso-Martinez, J.; Rodriguez-Amenedo, J.L. Comparison of Two Energy Management System Strategies for Real-Time Operation of Isolated Hybrid Microgrids. *Energies* **2021**, *14*, 6770. [CrossRef]
38. Yang, B.; Wang, J.; Zhang, X.; Wang, J.; Shu, H.; Li, S.; He, T.; Lan, C.; Yu, T. Applications of battery/supercapacitor hybrid energy storage systems for electric vehicles using perturbation observer based robust control. *J. Power Source* **2020**, *448*, 227444. [CrossRef]
39. Ren, G.; Wang, J.; Li, Y.; Zhang, G. Power distribution optimization of a fully active hybrid energy storage system configuration for vehicular applications. *J. Ind. Inf. Integr.* **2023**, *33*, 100459. [CrossRef]
40. Hassani, H.; Zaouche, F.; Rekioua, D.; Belaid, S.; Rekioua, T.; Bacha, S. Feasibility of a Standalone Photovoltaic/Battery System with Hydrogen Production. *J. Energy Storage* **2020**, *31*, 101644. [CrossRef]

41. Rekioua, D.; Bensmail, S.; Bettar, N. Development of hybrid photovoltaic-fuel cell system for stand-alone application. *Int. J. Hydrogen Energy* **2014**, *39*, 1604–1611. [CrossRef]
42. Yasin, A.M.; Alsayed, M.F. Fuzzy logic power management for a PV/wind microgrid with backup and storage systems. *Int. J. Electr. Comput. Eng.* **2021**, *11*, 2876–2888. [CrossRef]
43. Elmouatamid, A.; Ouladsine, R.; Bakhouya, M.; El Kamou, N.; Khaidar, M.; Zine-Dine, K. Review of Control and Energy Management Approaches in Micro-Grid Systems. *Energies* **2021**, *14*, 168. [CrossRef]
44. Olatomiwa, L.; Mekhilef, S.; Ismail, M.S.; Moghavvemi, M. Energy management strategies in hybrid renewable energy systems: A review. *Renew. Sustain. Energy Rev.* **2016**, *62*, 821–835. [CrossRef]
45. Ismail, M.S.; Moghavvemi, M.; Mahlia, T.M.I.; Muttaqi, K.M.; Moghavvemi, S. Effective utilization of excess energy in standalone hybrid renewable energy systems for improving comfort ability and reducing cost of energy: A review and analysis. *Renew. Sustain. Energy Rev.* **2015**, *42*, 726–734. [CrossRef]
46. Farhadi, M.; Mohammed, O. Adaptive energy management in redundant hybrid DC micro grid for pulse load mitigation. *IEEE Trans. Smart Grid* **2015**, *6*, 654–662. [CrossRef]
47. Meng, L.; Sanseverino, E.R.; Luna, A.; Dragicevic, T.; Vasquez, J.C.; Guerrero, J.M. Microgrid supervisory controllers and energy management systems: A literature review. *Renew. Sustain. Energy Rev.* **2016**, *60*, 1263–1273. [CrossRef]
48. Abedi, S.; Alimardani, A.; Gharehpetian, G.; Riahy, G.; Hosseinian, S. A comprehensive method for optimal power management and design of hybrid RES-based autonomous energy systems. *Renew. Sustain Energy Rev.* **2012**, *16*, 1577–1587. [CrossRef]
49. Robyns, B.; Davigny, A.; Saudemont, C. Methodologies for supervision of hybrid energy sources based on storage systems—A survey. *Math. Comput. Simul.* **2013**, *91*, 52–71. [CrossRef]
50. Erdinc, O.; Elma, O.; Uzunoglu, M.; Selamogullari, U.; Vural, B.; Ugur, E.; Boynuegri, A.R.; Dusmez, S. Experimental performance assessment of an online energy management strategy for varying renewable power production suppression. *Int. J. Hydrogen Energy* **2012**, *37*, 4737–4748. [CrossRef]
51. Mebarki, N.; Rekioua, T.; Mokrani, Z.; Rekioua, D. Supervisor control for stand-alone photovoltaic/hydrogen/ battery bank system to supply energy to an electric vehicle. *Int. J. Hydrogen Energy* **2015**, *40*, 13777–13788. [CrossRef]
52. Rekioua, D.; Rekioua, T. DSP-controlled direct torque control of induction machines based on modulated hysteresis control. In Proceedings of the 2009 13th 21th International Conference on Microelectronics, ICM 2009, Marrakech, Morocco, 19 December 2009; pp. 378–381. [CrossRef]
53. Pattnaik, S.; Kumar, M.R.; Mishra, S.K.; Gautam, S.P.; Appasani, B.; Ustun, T.S. DC Bus Voltage Stabilization and SOC Management Using Optimal Tuning of Controllers for Supercapacitor Based PV Hybrid Energy Storage System. *Batteries* **2022**, *8*, 186. [CrossRef]
54. Lemian, D.; Bode, F. Battery-Supercapacitor Energy Storage Systems for Electrical Vehicles: A Review. *Energies* **2022**, *15*, 5683. [CrossRef]
55. Lee, N.; Nee, C.H.; Yap, S.S.; Tham, K.K.; You, A.H.; Yap, S.L.; Mohd Arof, A.K.B. Capacity Sizing of Embedded Control Battery–Supercapacitor Hybrid Energy Storage System. *Energies* **2022**, *15*, 3783. [CrossRef]
56. Zubieta, L.; Bonert, R. Characterization of Double-Layer Capacitors (DLCs) for Power Electronics Applications. *IEEE Trans. Ind. Appl.* **2000**, *36*, 199–205. [CrossRef]
57. Zhang, L.; Hu, X.; Wang, Z.; Sun, F.; Dorrell, D.G. A Review of Supercapacitor Modeling, Estimation, and Applications: A Control/Management Perspective. *Renew. Sustain. Energy Rev.* **2018**, *81*, 1868–1878. [CrossRef]
58. Helseth, L.E. Comparison of methods for finding the capacitance of a supercapacitor. *J. Energy Storage* **2021**, *35*, 102304. [CrossRef]

Disclaimer/Publisher's Note: The statements, opinions and data contained in all publications are solely those of the individual author(s) and contributor(s) and not of MDPI and/or the editor(s). MDPI and/or the editor(s) disclaim responsibility for any injury to people or property resulting from any ideas, methods, instructions or products referred to in the content.